NASA CR-54991
PWA-2845

# THIRD QUARTERLY REPORT

# BRAYTON-CYCLE TURBOMACHINERY ROLLING-ELEMENT BEARING SYSTEM

prepared for
National Aeronautics and Space Administration

May 1966

Contract NAS3-7635

National Aeronautics and Space Administration
Lewis Research Center
21000 Brookpark Road
Cleveland, Ohio
W. Ream



Prepared by Herbert Means H. Means, Proj. Engineer
Approved by P. Bolan P. Bolan, Prog. Manager

Pratt & Whitney Aircraft
DIVISION OF UNITED AIRCRAFT CORPORATION
EAST HARTFORD, CONNECTICUT

# FOREWORD

This report describes the progress of the work conducted between January 2 and April 2, 1966 by the Pratt & Whitney Aircraft Division of United Aircraft Corporation, East Hartford, Connecticut, on Contract NAS3-7635, Brayton-Cycle Turbomachinery Roller-Contact Bearings, for the Lewis Research Center of the National Aeronautics and Space Administration. The objective of the program is to design and demonstrate performance of a rolling-element bearing system for the Brayton-cycle turbomachinery being developed under Contracts NAS3-4179 and NAS3-6013.

# TABLE OF CONTENTS

# LIST OF FIGURES

# I. SUMMARY

This report presents the work completed during the third three-month period of a design and experimental program formulated to investigate the potential of an oil-lubricated rolling-element bearing system for Brayton-cycle space power machinery. The technical progress, the work accomplished and the program status for the third quarterly period, January 2 through March 2, 1966, are presented.

During the previous report period the analysis of the rolling-element lubrication system was completed. Analyses of alternate systems which offer less technical risk at the expense of higher power consumption were also completed. Designs of the turbine-compressor and turboalternator on rolling-element bearings were completed during this report period. The designs of the experimental apparatus which will be used to investigate the features of the lubrication systems were also completed and fabrication was initiated. Laboratory evaluation of candidate adsorbate materials included a 100-hour test of 13X molecular sieve pellets with satisfactory results.

## II. INTRODUCTION

In the application of the Brayton cycle to space power sources, two types of rotor support systems are being considered and evaluated by the National Aeronautics and Space Administration. In one case, the rotating components are supported by gas bearings and the cycle working fluid is used as lubricant and bearing coolant. In the other case, the rotors are supported by rolling-element bearings which are lubricated and cooled by oil.

The specific Brayton-cycle machinery considered in this program consists of a turbine-driven compressor and a turbine-driven alternator. These units are being designed and constructed utilizing gas bearings under Contracts NAS3-4179 and NAS3-6013. The gas bearing version of this machinery is shown in Figure 1. The cycle flow enters the compressor at 76°F through the inlet duct around the housing which contains a thrust bearing and a radial bearing. The argon is compressed in the six-stage axial-flow compressor and then flows through the radial diffuser exit scroll and ducting. The argon is heated to 1490°F outside of the unit and is returned to the turbine inlet ducting and scroll. A second radial gas bearing is located between the compressor exit and turbine inlet. The argon flows through the single-stage axial-flow turbine which drives the compressor at 50,000 rpm. It then exhausts through the exit ducting which connects to the two-stage alternator-drive turbine. The 4-pole alternator is driven at 12,000 rpm and is supported by bearings on each side. After passing through the alternator-drive turbine, the argon exhausts through the exit scroll and ducting. It is cooled outside of the machinery and returned to the compressor inlet.

The vast majority of Brayton-cycle powerplants in use in the world today employ rolling-contact oil-lubricated bearings. In the application of Brayton-cycle machinery to the space environment, several significant questions require investigation to determine if rolling-element bearings can provide a satisfactory rotor support system for this application:

1) Can rolling-element bearings provide the endurance capability with the high reliability required in space applications for a nominal mission time of 10,000 hours?

2) Can the lubricant be cooled and circulated in a zero-gravity environment?

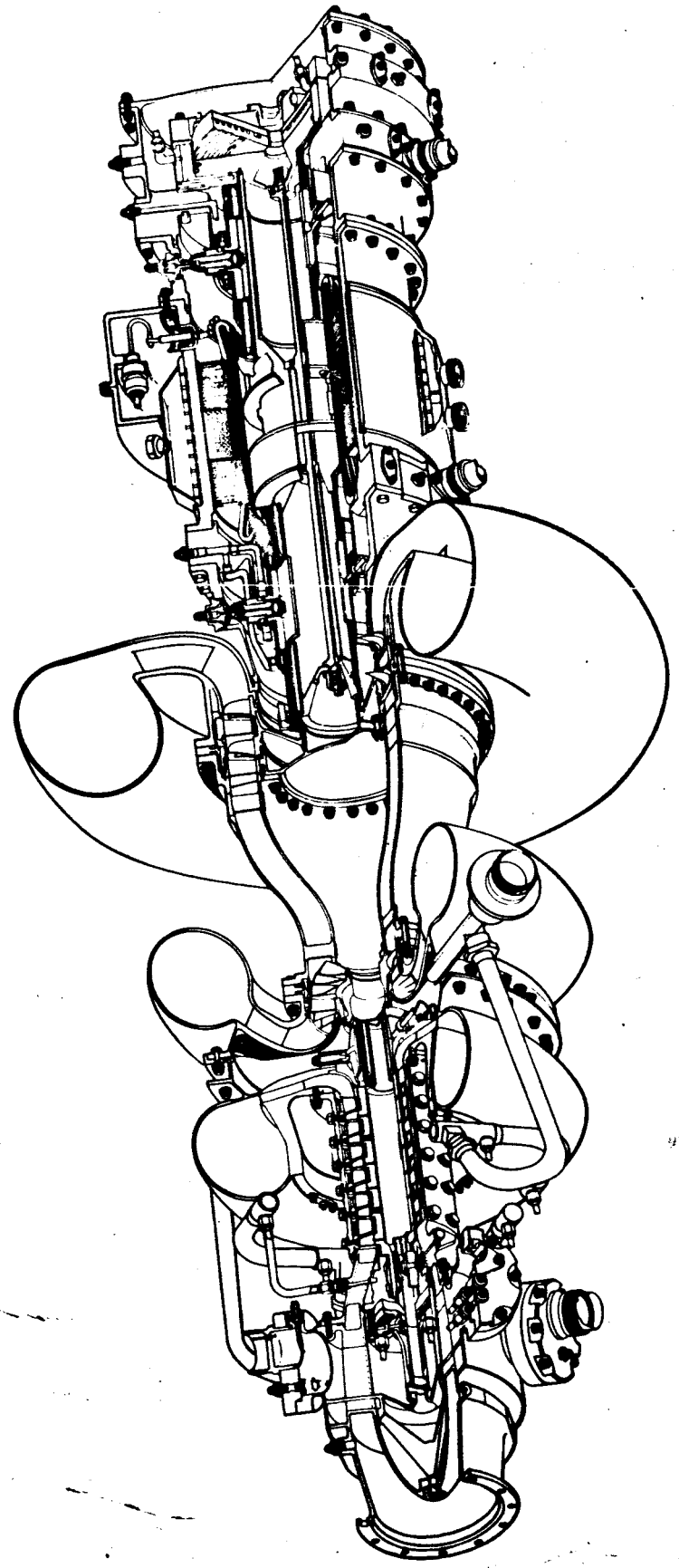

Figure 1 Brayton-Cycle Turbomachinery Employing Gas Bearings (Contracts NAS3-4179 and NAS3-6013)

3) Can the lubricant system and bearing cavities be sealed with low parasitic power losses by components with the required life capability?

4) Can the lubricant be prevented from contaminating the cycle working fluid (argon)?

The purpose of this program is to design and demonstrate the performance of a rolling-element bearing system for the turbine-compressor and turboalternator being developed under Contracts NAS3-4179 and NAS3-6013. The components of this rolling-element bearing system are bearings, seals, lubrication system and gas cleanup system. The work consists of the following four phases:

1) Design of a rolling-element bearing system that retains components of the turbine-compressor and turboalternator (designed under Contracts NAS3-4179 and NAS3-6013) to as great an extent as practical with no alteration in aerodynamic design. The shaft support system is intended to achieve low parasitic losses commensurate with high reliability for the full mission life.

2) Design and fabrication of component test rigs.

3) Conduct bearing, seal, scavenge separator and adsorber performance tests.

4) Conduct a pilot endurance demonstration of the rolling-element bearing system.

Although the rolling-element bearing system encompasses the turboalternator as well as the turbine-compressor, only the rolling-element bearing system components for the turbine-compressor will be investigated experimentally. The separator, which is an integral part of the turboalternator, will be evaluated in a separate test rig as will the residual oil adsorber.

## III. TURBINE-COMPRESSOR DESIGN

The purpose of the turbine-compressor design task is to provide a rolling-element bearing system design that can be employed as an alternate to the gas-bearing system being developed to support the turbine-compressor rotor under Contract NAS3-4179. The basic objectives and considerations for this design are 1) to use a bearing, seal, and lubrication system that provides endurance capability for a mission time of 10,000 hours with a high reliability potential, 2) to use a bearing, seal, and lubrication system that has acceptable parasitic losses, and 3) to develop a mechanical design that utilizes the existing turbine-compressor aerodynamic design developed under Contract NAS3-4179 with minimum alterations.

In the first quarterly report[1], the general arrangement of the turbine-compressor with rolling element bearings was evolved and the detailed analysis of the preloaded ball bearings was presented. In the second quarterly report[2], the detailed analyses of the rotor dynamics were described and thermal analyses of the bearing areas were presented. Also, the candidate seals were discussed. During this report period, the design of the turbine-compressor on rolling-element bearings was completed. This section presents a brief description of the turbine-compressor design and additional design information including significant stresses, material selections and clearances. A further discussion of the seals is also included.

The Brayton-cycle axial-flow turbine-compressor consists of a six-stage compressor driven by a single-stage turbine at a design speed of 50,000 rpm. The turbine-compressor design incorporating rolling-element bearings is shown in Figure 2. Argon enters the compressor at 76°F through a duct which houses the No. 1 bearing compartment. The working fluid discharges radially into a scroll and then is piped to the heat source. The hot argon (1490°F) is returned to the single-stage axial turbine through an inlet scroll and then the gas flows through an annular diffuser to the alternator drive turbine. The No. 2 bearing compartment is located inside the exit diffuser downstream of the turbine. The compressor and turbine blading, the outer casings, and the inlet and exhaust ducts and scrolls, are essentially identical to those for the gas-bearing design. The rotor is of drum construction with the turbine blades and disk integral. An integral shaft extension serves as the support of the No. 2 bearing. The No. 1 bearing is mounted on a separable extension of the shaft. The two bearing compartments are similar in design. Each contains a counterbore angular-contact ball bearing lubricated by a mixture of oil mist and argon, and cooled by

[1]Numbered references are listed in Appendix 1.

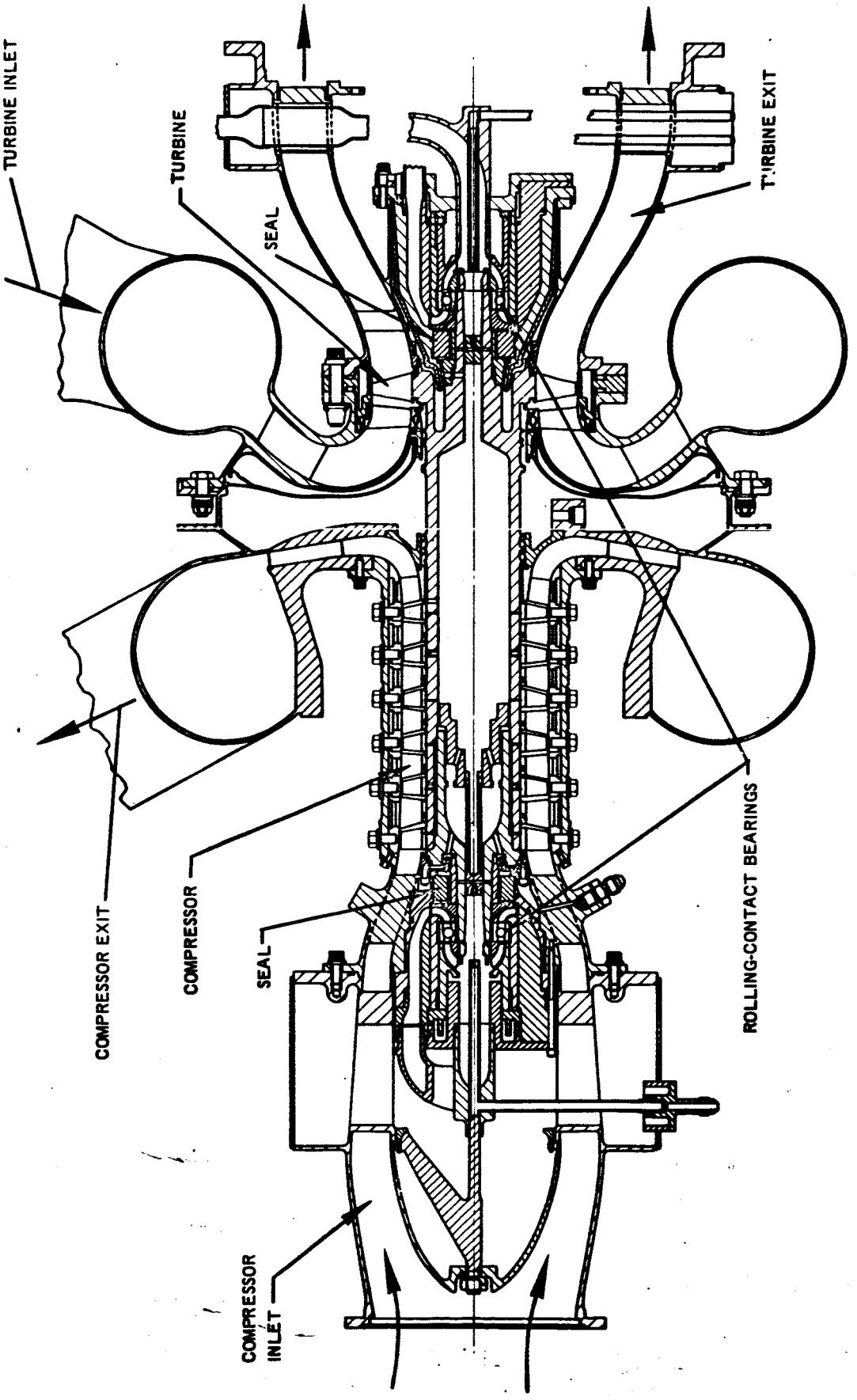


Figure 2 Brayton-Cycle Turbine-Compressor with Rolling-Contact Bearings

oil supplied through the shaft and flowing through grooves in the inner race of the bearing. The cooling oil passes through the rotating sealplate to cool the face seal. The oil and the oil-argon mixture are pumped from the bearing area by impeller blades on the back surface of the sealplate. The bearings are supported by an oil film in a small annular gap in the bearing housings. This oil film provides squeeze film support and damping. This method of support also permits axial motion of the No. 1 bearing housing which is spring-loaded. As a result the bearings are preloaded in thrust to assure skid-free operation under all conditions.

In the gas-bearing version of the turbine-compressor, the significant stresses were analyzed. The rolling-contact bearing version of this unit employs many of the same parts subjected to the same conditions as in the gas-bearing configuration. Therefore, the stresses are identical and the design margins are the same. A number of areas are modified to accommodate the rolling-contact bearing rotor-support system and a summary of significant stresses in these areas is presented in Table 1. The allowable stress presented in Table 1 is generally the yield strength of the material. However, in the compressor drum the allowable stresses are based on burst considerations, while creep is the criterion in the turbine.

TABLE 1

Turbine-Compressor Significant Stresses

| Part | Material | Allowable Stress, psi | Calculated Stress, psi |
|---|---|---|---|
| tie bolt | AMS-5660 | 100,000 | 12,700 |
| compressor drum, 1st stage | PWA-1007 | 119,300 | 32,500 |
| compressor drum, 2nd stage | PWA-1007 | 118,600 | 29,200 |
| compressor drum, 3rd stage | PWA-1007 | 117,300 | 29,250 |
| compressor drum, 4th stage | PWA-1007 | 116,600 | 26,250 |
| compressor drum, 5th stage | PWA-1007 | 115,900 | 26,000 |
| compressor drum, 6th stage | PWA-1007 | 115,200 | 25,900 |
| turbine disc, front | PWA-1007 | 115,000 | 98,000 |
| turbine disc, rear | PWA-1007 | 110,000 | 88,000 |
| bearing retainer nut | AMS-6304 | 130,000 | 3,700 |
| bearing housing | AMS-6304 | 130,000 | 15,400 |
| bearing thrust springs | AMS-5688 | 100,000 | 52,600 |
| main shaft flange | AMS 5660 | 100,000 | 13,700 |
| main shaft spline | AMS-5660 | 100,000 | 11,000 |
| main shaft hub | AMS-5660 | 100,000 | 10,200 |

The materials selected for the rolling-contact bearing version of the turbine-compressor are identical with the gas-bearing version as far as possible. For example, the turbine and integral shaft is the same high-temperature nickel alloy in both cases. The use of the same materials in both designs is important for maintaining interchangeability and in order to restrict the areas requiring redesign. Where new selections were required in the bearing areas, the materials were selected for suitability for the function and compatibility and fit with adjoining parts. The calculated rotor weight in the oil-bearing design is slightly higher than in the corresponding gas-bearing design: 11.73 and 10.64 pounds, respectively. The weight of the complete turbine-compressor on rolling-element bearings is 223 pounds.

Of necessity, there are some differences in mechanical arrangement between the rolling-contact bearing turbine-compressor and the gas-bearing version. The most significant is the method of fixing the axial location of the shaft. In the gas-bearing configuration, the thrust bearing is located at the compressor inlet (the No. 1 location) while in the rolling-contact bearing unit the axial position of the shaft is fixed by the ball bearing at the turbine discharge (the No. 2 location). Since preloaded ball bearings are employed, the spring-loaded bearing must be free to move axially to accommodate differences in thermal expansion and thermal transients. The limited space available restricted the location of the spring to the upstream side of the bearing in the No. 1 position and the downstream side in the No. 2 position. The turbine-compressor may be installed in the launch vehicle in the vertical position with the compressor end up. During launch, even though the rotor is stationary, the bearings must maintain the rotor position. Since accelerations of up to 4.6 g are anticipated, the bearings will have to support a thrust load of about 54 pounds. If the spring which preloads the bearing were at the turbine discharge, and if the spring had a low spring rate, the thrust on the rotor would be supported on the counterbore side of the No. 1 bearing. Since only a very small shoulder exists on the counterbore side of the outer race to permit assembly of the bearing, this launch load might damage the bearing. Therefore, the bearing preload springs are applied to the No. 1 bearing and the No. 2 bearing is fixed. With the shaft located axially at the turbine exit, the axial clearances in the compressor were examined. With a nominal axial clearance of 0.080 inch cold, the minimum axial clearance in the compressor is 0.030 inch due to thermal transients and tolerances.

The radial position of the shaft is fixed by different techniques in the rolling-contact bearing turbine-compressor compared with the gas-bearing design. In the gas-bearing machinery as presently contemplated,

proximity probes are included and the radial positions of the bearings are adjustable. Therefore, the bearings can be adjusted after assembly to center the shaft based on the probe data. No provisions for bearing radial position adjustments are included in the rolling-contact bearing version. In this version, the bearing outer housing is supported by a thin oil film and the second quarterly report indicated that rotor excursions of about 0.0004 inch are predicted from the dynamic analyses. The number of fits between mating parts is different in the two designs and allowance must be made for the tolerance buildup as a result. The radial clearances of the labyrinth seals and blade tips were examined for the rolling-contact design and clearances 0.001 to 0.002 inch larger are required depending on location, than are required in the gas-bearing turbine-compressor.

In the second quarterly report the four candidate seal designs were described and during this report period, further details were established. The four candidate seals are 1) a dry-face seal with damped-bellows secondary seal, 2) a wet-face seal with damped-bellows secondary seal, 3) a hydrodynamic-lift face seal with damped-bellows secondary seal, and 4) a controlled-clearance ring seal, also called a floating labyrinth seal.

The detail design of the dry-face seal was developed. The seal diameter was made as small as possible to achieve lowest power consumption and leakage with greatest durability. A mean seal face diameter of 1.53 inches was chosen to avoid undue restriction of the shaft outside diameter which results in a mean rubbing velocity of 335 ft/sec. To provide the most positive protection against oil leakage across the contact face, the choice was made to have the oil at the outer edge of the rotating interface so that any leakage must oppose the centrifugal force of the rotating members.

The choice of seal contact load is a function of seal dynamics, seal lip width, and contact pressure. For the seal diameter selected and a seal face runout of 0.0005 inch FIR the maximum acceleration of a point on the seal is 18 g. The weight of the seal assembly which must respond to the sealplate runout is 0.065 lb. The minimum allowable load on the seal interface is the product of 18 g and 0.0065 lb, or 1.2 lb. The selected seal lip width is approximately 0.080 inch. The contact pressure on the seal face at 1.2 lb load is 3 psi. The choice of maximum seal contact load is largely a function of seal power consumption and durability. The value of 2.25 lb selected results in a maximum power consumption of 200 watts at a coefficient of friction of 0.2. Seal wear rates are extremely difficult to predict but an allowance of 0.030 inch is provided.

The choice of bellows spring rate is largely dictated by space restrictions and the maximum pressure differential. The pressure and diametral limitations dictate a bellows wall thickness of 0.003 inch. Eleven full convolutions were selected to provide a bellows stiffness of 21.2 lb/inch which provides a satisfactory spring rate without placing serious demands on the space restrictions. A circumferential spring-loaded strip applied to the outside of the bellows convolutions provides damping.

The wet-face seal is similar to the dry-face seal except that a small quantity of oil is fed to the contact area between the carbon and the rotating plate. The details of the wet-face seal design are similar to those of the dry-face seal except that the seal lip width is increased to 0.200 inch to provide area for the oil film and the oil feed holes. The mean diameter at the wet seal face is 1.422 inches and the mean rubbing velocity is 311 feet per second. The wear of the wet-face seal should be significantly less than the dry-face seal and the power consumption should be somewhat lower.

Three seal configurations will be evaluated experimentally in the bearing-seal-scavenge rig. In addition to the dry-face seal and wet-face seal, two candidate seal designs were considered for experimental evaluation as the third seal. One was a face seal, Figure 3, which used spiral grooves in the contact zone on the plate to provide hydrodynamic lift.

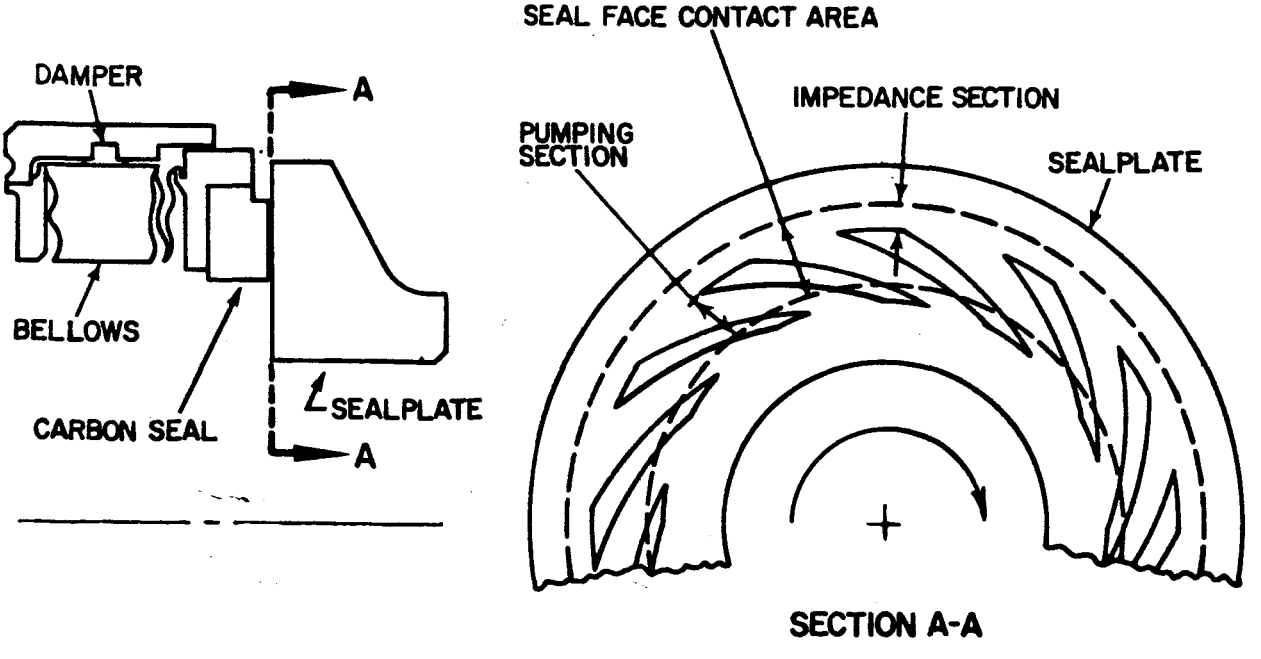


Figure 3 Hydrodynamic Face Seal

The advantage of this lifting action is to reduce the contact force between the carbon and the plate, reducing both friction and wear. Data was presented in the second quarterly report on the load-carrying characteristics and gas-film stiffness in terms of gas-film thickness for a hydrodynamic face seal in the turbine-compressor. During this period, a potential hydrodynamic face seal analytical design was selected for this application. The basic arrangement of this seal is identical with the wet-face seal. The same damped bellows serves as the secondary seal. The low-pressure argon and oil are located on the outside of the seal while the high-pressure gas is inside. In order to provide radial space for the spiral grooves, the seal lip width of 0.200 inch was retained and the same mean diameter was selected. An outward pumping configuration was chosen to minimize gas and oil leakage and to provide high film stiffness. The carbon lip extends 0.061 inch radially outward beyond the spiral grooves to provide a circumferential dam at the outer edge of the contact area (called "impedance section" on Figure 3). A gas film thickness of 0.0003 inch was selected to provide margin between the seal resonant frequency and the shaft rotational frequency. Twelve spiral grooves of 0.00095 inch depth were selected. These grooves are at an angle of 71.7 degrees to the radial direction. The predicted power consumption of the hydrodynamic face seal is 31 watts.

The other type considered is a controlled-clearance ring seal, or floating labyrinth seal, shown in Figure 4. This seal consists of a carbon ring with close radial clearance with the shaft. The ring is free to move axially and, when gas pressure is applied, bears against a static wall. In order to provide a shutdown seal, the static wall is supported by a bellows which acts as a static seal and as a spring to close the seal against a retaining plate on the shaft when no gas pressure is applied. There are two advantages to this seal, 1) since the carbon does not continuously rub against a rotating part, the predicted heat generation is only about 15 watts, 2) the bellows is essentially static during normal operation and does not have to deflect to follow runout as in the case of a face seal. Therefore, the possibility of bellows fatigue is reduced. The controlled-clearance ring seal was selected as the third seal configuration for test.

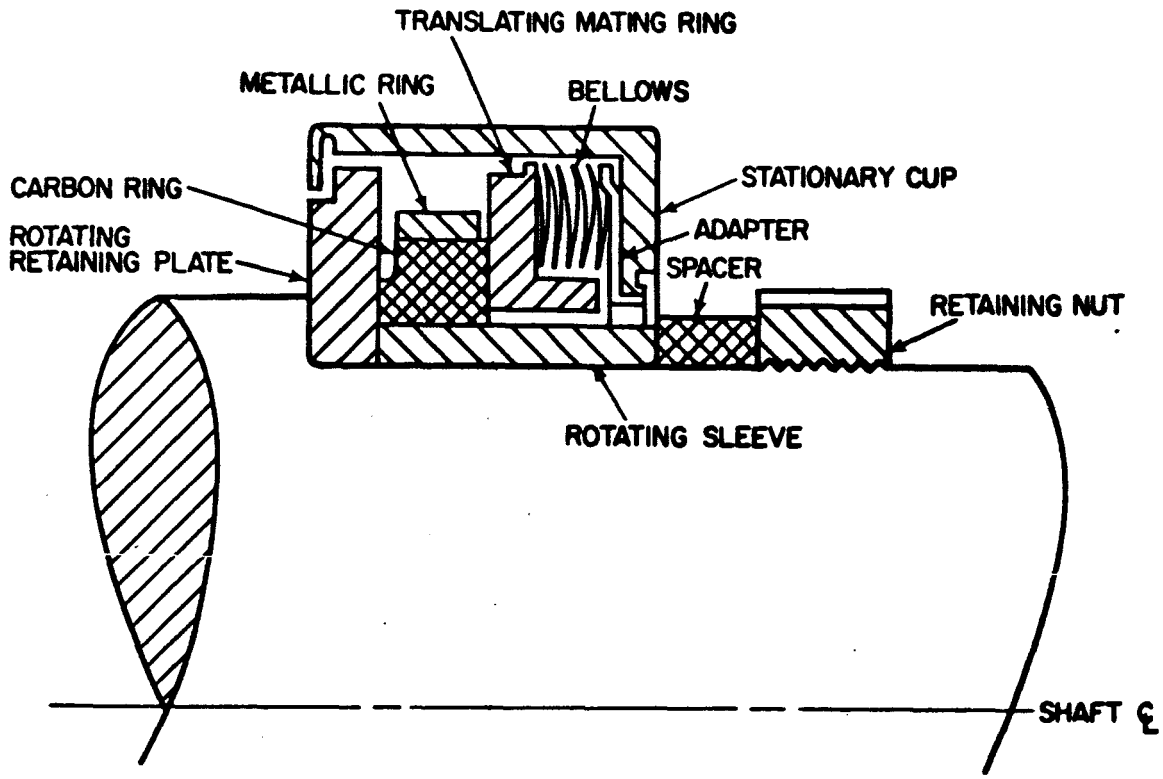


Figure 4 Controlled-Clearance Ring Seal

In the previous report several rolling-element bearing lubrication systems were considered for the Brayton-cycle turbomachinery. For the low-loss systems examined, scavenge pumps in the bearing compartments were required to make up the loss in pressure suffered by the mixtures of argon and oil circulating through the system. One concept, shown in Figure 2, is to utilize an impeller on the back face of the sealplate to pump argon, which in turn would drag the oil through the system. This configuration is estimated to be marginal when operating in a vertical position on the ground; therefore, a second configuration based on the jet pump principle was also considered.

During this report period the jet scavenge pump concept was developed further and a preliminary design was evolved. This scavenge pump uses the energy imparted to the oil by the rotation of the shaft. The oil passes through passages in the shaft and associated rotating parts to remove heat from the bearing and the seal. The jet pump effect is achieved by directing the oil discharged from the rotating shaft into a narrow radial passage which serves as the throat of the jet scavenge pump. Argon is drawn into the throat at a velocity lower than that of the oil.

The oil and argon mix in the throat and a reduction in momentum in the oil is accompanied by a static pressure increase in the argon.

A cross-section of the scavenge pump is shown in Figure 5. One concern in the design of this pump is the potential difficulty in obtaining nearly equal argon flow rates on either side of the oil jet. Since the seal leakage is not a significant part of the argon flow, some circulating argon flow is brought through the passages in the sealplate to the seal side of the oil jet to provide symmetric flow at the pump inlet. The flow passages through the sealplate impeller are backward-sloping with respect to rotation. Small radial diffuser vanes are incorporated to provide the best possible argon flow characteristics at the pump inlet and to convert some of the kinetic energy in the argon to static pressure. There will be a pressure loss in the argon passing through the passages and, to preserve symmetry, similar argon flow passages are provided on the bearing side of the scavenge pump. The effect of the impeller and the vanes is a pressure loss of 0.3 psi in the argon prior to entering the jet pump. With a tip diameter of 2.12 inches for the oil impeller and a conservative throat width of 0.09 inch, the theoretical jet pump rise in the argon is 1.35 psi. Therefore, the predicted overall static pressure rise in the argon is 1.05 psi. This is more than twice the argon pressure rise anticipated in the previous configuration.

The performance of the jet pump is particularly dependent upon the width of the radial slot (throat). Throat widths in the range of 0.045 to 0.09 inch are practical for this design. If the throat width of 0.045 inch were employed, a static pressure rise of over 2 psi would be possible. A radial throat length of 0.2 inch is equivalent to a throat length over 0.5 inch in the flow direction (because of the tangential oil discharge), and is sufficient to provide essentially the full static pressure rise that is potentially available. The jet pump discharge collector is designed to be compatible with the axial orientation of the discharge pipe in the turbine-compressor. In order to permit throat width adjustments, the collector scroll has a cross-sectional area which varies with angular position by varying the axial dimension while maintaining radial dimensions. The resulting shape of the wall on the discharged side of the collector is an axial spiral.

The estimated performance of the jet pump is presented graphically in Figures 6, 7, and 8, which define the predicted pressure rise-argon flow characteristics for three throat widths and two equivalent throat lengths. Figures 6, 7, and 8 do not include the pressure losses introduced by the argon passing through the access holes in the rotating plate. A summary of the design relations for the jet scavenge pump is presented in Appendix 2.

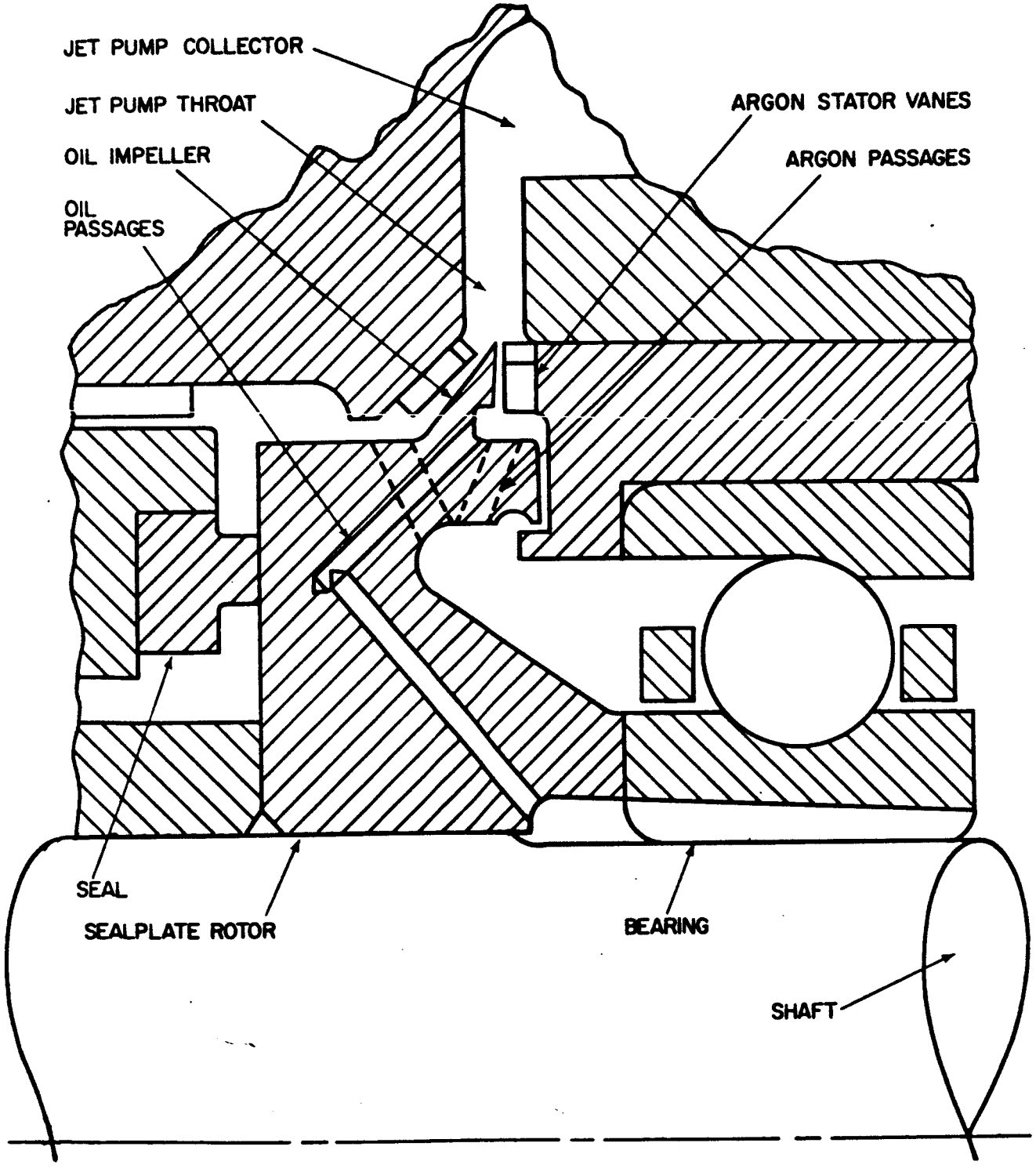


Figure 5 Annular Jet Pump Scavenge System

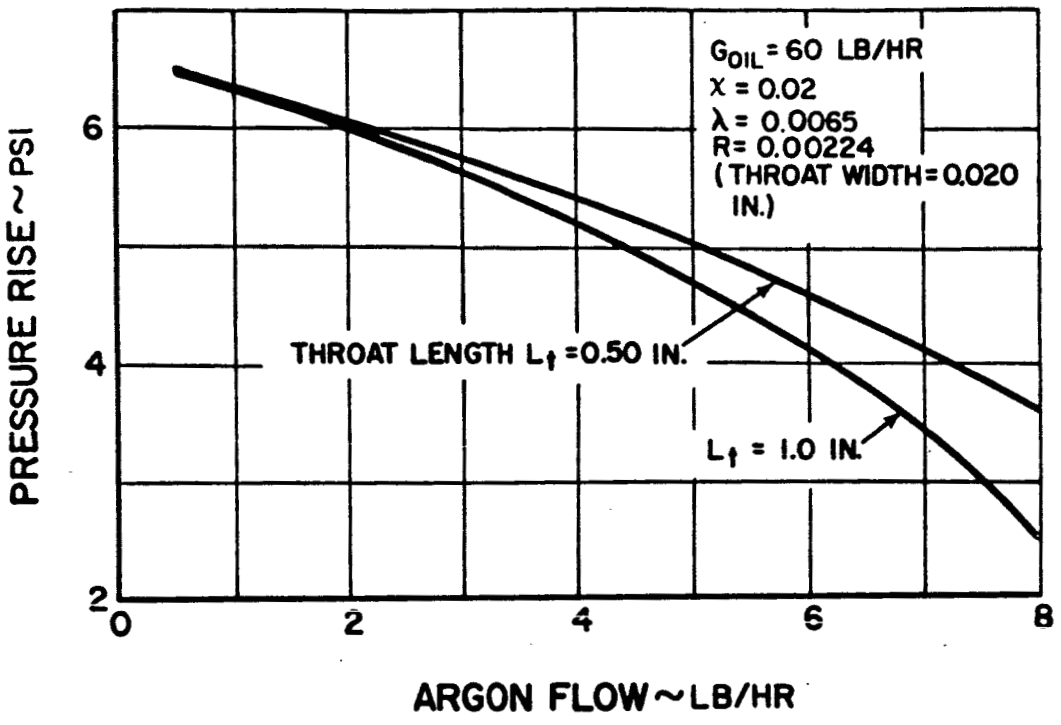


Figure 6 Pressure-Flow Characteristics of Annular Jet Scavenge Pump for Turbine-Compressor

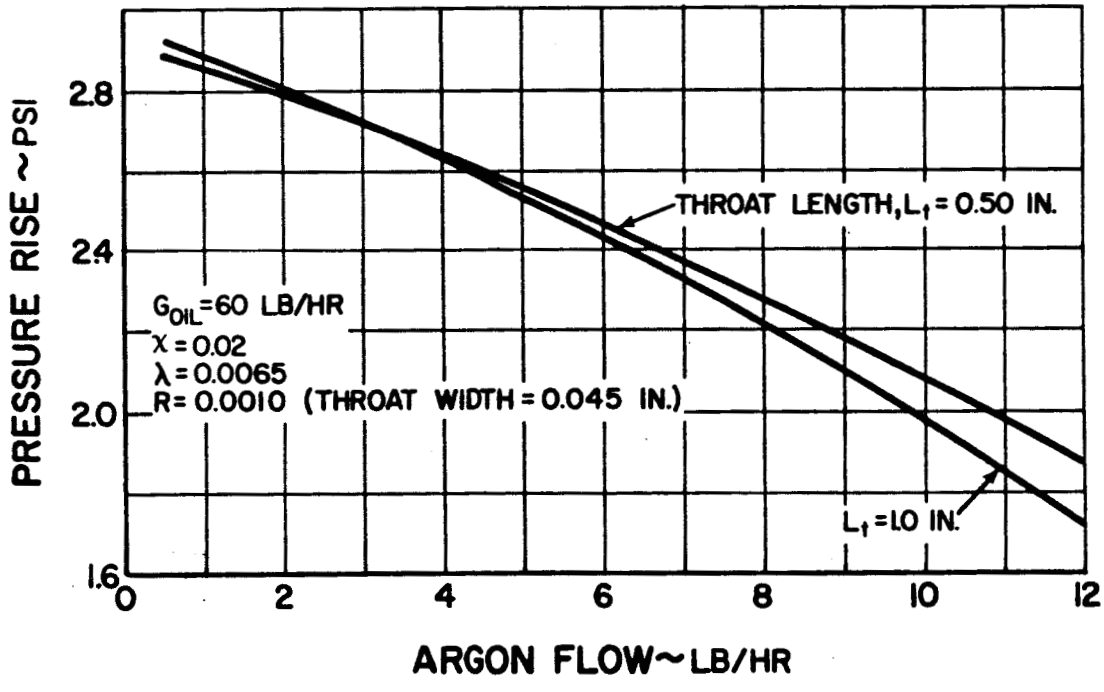


Figure 7 Pressure-Flow Characteristics of Annular Jet Scavenge Pump for Turbine-Compressor

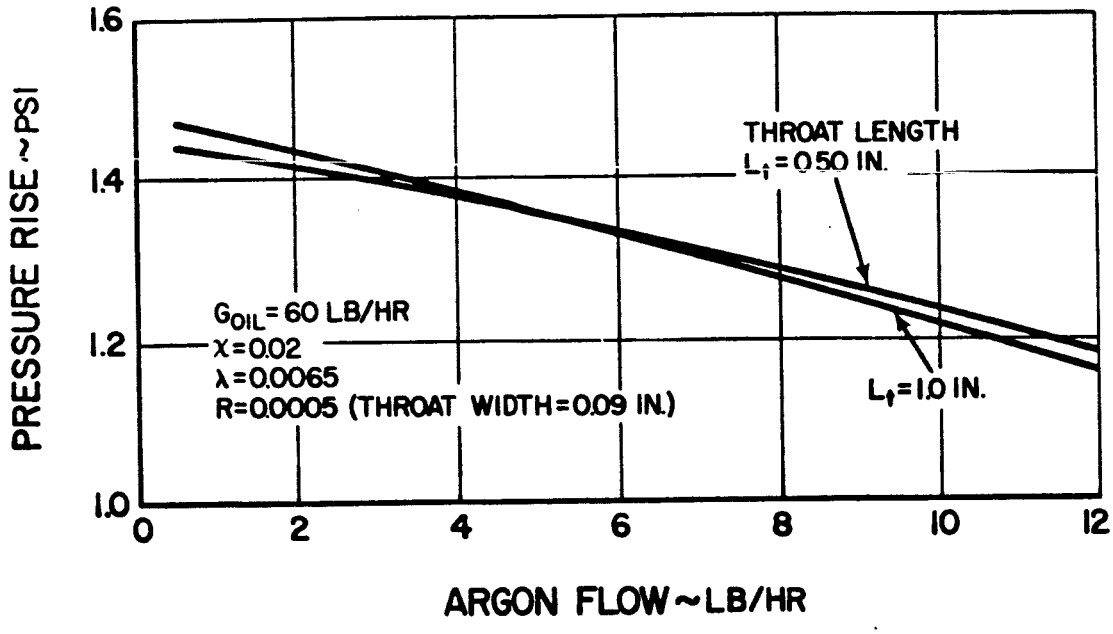


Figure 8 Pressure-Flow Characteristics of Annular Jet Scavenge Pump for Turbine-Compressor

# IV. TURBOALTERNATOR DESIGN

The turboalternator design task, like the turbine-compressor task discussed in Section III, is to design a rolling-element bearing system which can be utilized as an alternate to the gas-bearing turboalternator design produced under Contract NAS3-6013. Similarly, the design objectives and considerations are 1) to use a bearing, seal, and lubrication system that provides endurance capability for a mission time of 10,000 hours with a high reliability potential, 2) to use a bearing, seal, and lubrication system which has acceptable parasitic losses, and 3) to develop a mechanical design which utilizes the existing turboalternator aerodynamic and electric design developed under Contract NAS3-6013 with minimum alterations.

In the first quarterly report, the general arrangement of the turboalternator with rolling-element bearings was evaluated and preliminary rotor dynamics were considered which included the effects of the overhung oil-gas separator. In the second quarterly report, details of the oil-gas separator were developed and thermal maps of critical areas were determined. Refinements were incorporated in the rotor design including the bearing and seal areas. During this report period, the design of the turboalternator for operation on rolling-element bearings was completed. A description of the overall design and additional detail design information concerning material selections, critical stresses, characteristics of the bearings, and critical speeds is presented.

The turboalternator consists of a four-pole brushless inductor alternator which operates at 12,000 rpm to produce 400-cycle per second, 3-phase electric power. The alternator stator is cooled by liquid circulated in the stator housing. A two-stage axial-flow turbine drives the alternator. The turbine receives argon at approximately 1225°F from the discharge of the turbine-compressor turbine through an annular transition duct, after passing through the alternator drive turbine, the argon exhausts through the exit scroll and ducting.

The design of the turboalternator on rolling-element bearings is presented in Figure 9. The alternator rotor is straddle-mounted between two rolling-element bearings with the turbine overhung from one end and the centrifugal argon-oil separator overhung from the other end. Between the alternator and the turbine, the shaft is supported by a roller bearing. The ball bearing between the alternator and the gas-oil separator provides radial support and also supports the thrust load imposed on the rotor. In order to minimize windage losses, the alternator cavity is maintained at approximately 6 psia with argon fed from the discharge of the gas-oil separator.

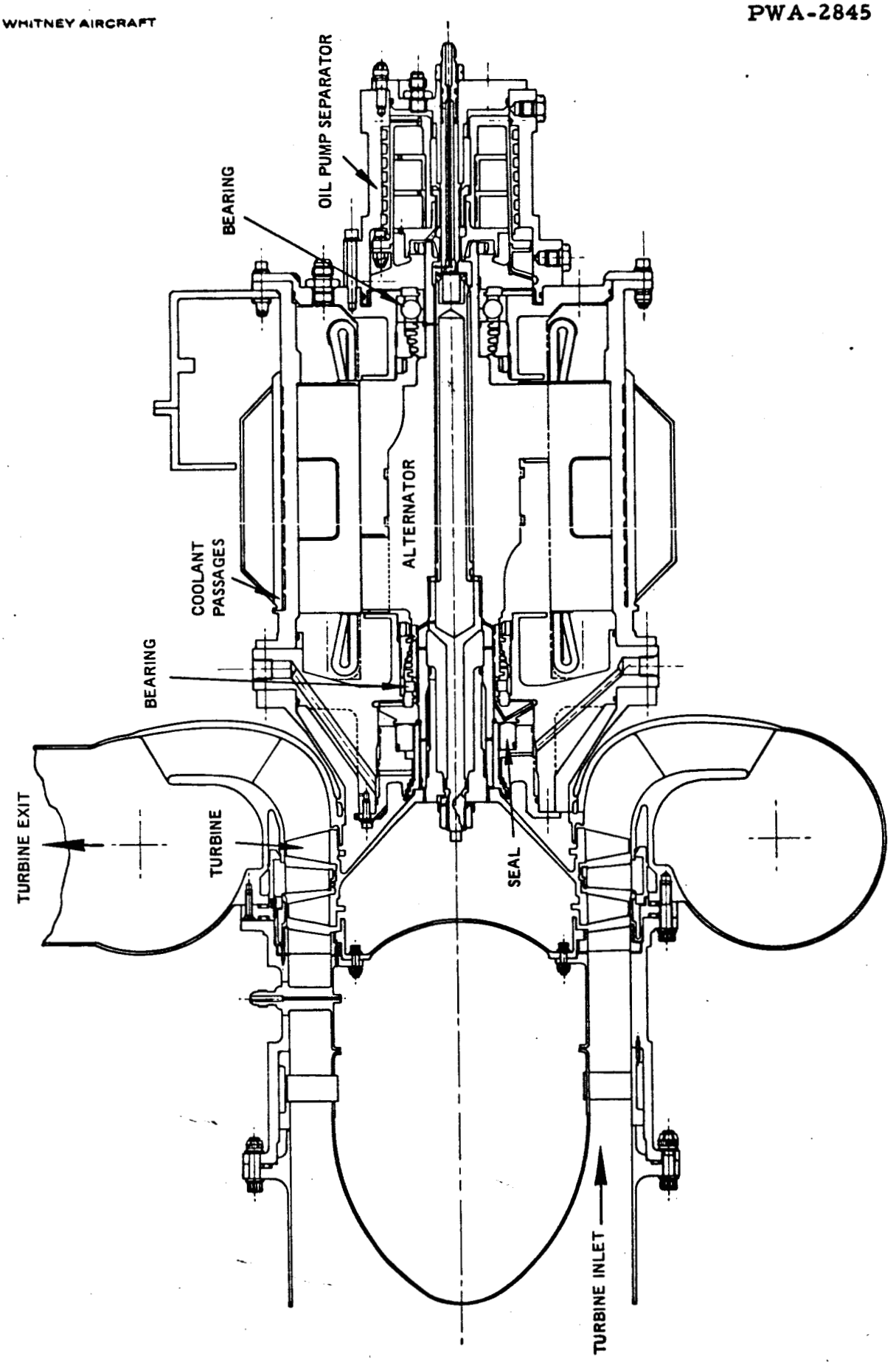


Figure 9 Brayton-Cycle Turboalternator with Rolling-Contact Bearings

The alternator cavity is separated from the bearing cavities by labyrinth seals which permit some leakage of argon into the bearing cavities. The gas-oil separator is arranged so that no rotating contact seal is required on that end of the machine. On the turbine end of the alternator shaft, a face seal similar in design to the face seals used in the turbine-compressor is provided. Argon bled from the compressor discharge pressurizes the face seal and also provides a small gas flow through a labyrinth seal past the turbine disc into the turbine gas path, which prevents hot gas from entering the area adjacent to the turbine disc.

The turboalternator on rolling-element bearings employs many of the same components operating in the same environment to the same stress levels as in the gas-bearing configuration. However, a number of alterations to the gas-bearing design were required. In order to reduce the linear speed of the bearing and the seal and to reduce the associated heat generated, the roller bearing is smaller in diameter than the gas bearing. Therefore, in order to permit assembly, the turbine disc has been modified in comparison to the gas-bearing configuration. Also, the gas-oil separator and oil pump on the free end of the alternator have no counterpart in the gas-bearing version. Many of the stresses are the same as in the gas-bearing design. However, a number of stresses were changed and these are summarized in Table 2. The material selections are consistent with the gas-bearing alternator wherever possible and these are also shown in Table 2. As Table 2 indicates, ample design margins are provided for the turboalternator on rolling-element bearings, based on 0.2 per cent yield criteria for each material.

TABLE 2
Turboalternator Significant Stresses

| Part | Material | 0.2% Yield, psi | Calculated Stress, psi |
|---|---|---|---|
| front bearing shroud | AMS 5667 | 100,000 | 32,500 |
| front bearing support | AMS 5667 | 100,000 | 49,000 |
| front tiebolt | PWA 1202 | 120,000 | 52,000 |
| shaft at rear bearing | AMS 6415 | 90,000 | 59,950 |
| rear shaft nut | AMS 5616 | 110,000 | 67,000 |
| rear seal | AMS 5667 | 100,000 | 14,000 |
| front retainer nut | AMS 5667 | 100,000 | 37,000 |
| rear bearing support | AMS 5667 | 100,000 | 69,100 |
| rear bearing inner race (axial compression) | M-50 | 323,000 | 30,750 |
| separator housing | AMS 4928 | 110,000 | 21,400 |
| separator bolt | AMS 4928 | 110,000 | 55,650 |
| separator dividers | AMS 4928 | 110,000 | 18,900 |
| separator dowel pins | AMS 5132 | 85,000 | 44,000 |
| separator oil scoop | AMS 5570 | 25,000 | 1,730 |

In addition to the stress analyses, deflections were analyzed in critical areas. The most critical portion of the turboalternator design is the overhung separator on the free end of the shaft. The analysis of this area included a pessimistic assumption for unbalance due to maldistribution of oil in the separator. The resulting deflections are predicted to be small and ample clearances are provided.

A ball bearing located between the alternator and the separator provides radial support and locates the shaft axially. In order to incorporate a full ball complement in the bearing, to provide for a one-piece retainer and to simplify assembly, a split-inner-ring ball bearing was selected. The design characteristics of the selected ball bearing are summarized as follows:

| | |
|---|---|
| Bearing Type | Angular-contact ball bearing with split inner ring |
| Oil System | Axial cooling slots on bore of inner ring |
| Bearing Size | 40mm bore diameter<br>80mm outer diameter<br>18mm wide |
| Internal Geometry | 11 balls of 0.500 inch diameter<br>2.40 inches pitch diameter<br>25-degree mounted contact angle<br>53 per cent inner race conformity, 52 per cent outer race conformity |

As in the turbine-compressor ball bearings, consumable-electrode vacuum-melted M-50 tool steel was selected for the balls and rings.

The thrust load on the rotor due to electromagnetic forces is very small. However, the thrust load due to aerodynamic forces is approximately 70 pounds at the design conditions. The rotor weighs 44.7 pounds and, for ground operation with the turbine end up, the thrust load on the bearing will be 115 pounds. The radial load on the ball bearing due to magnetic forces should be less than 20 pounds, and the mechanical unbalance radial force should be less than 2 pounds. In the unlikely event that the oil in the separator were to well up on one side, a radial load of up to 35 pounds might be applied to the ball bearing. Therefore, the maximum radial load which can be envisioned in space operation is about 55 pounds, but the anticipated radial load is less than 20 pounds.

Operation in the horizontal position on the ground will increase the radial force at this location due to the weight of the rotor by 22 pounds.

The ball bearing provides a predicted B-1 life well in excess of 10,000 hours over the range of load conditions anticipated. The predicted bearing life as a function of radial load, at the design thrust load of 70 pounds, is presented in Figure 10. The use of a split inner ring implies that the possibility exists for a bearing to wipe the unloaded half of the inner race. This bearing can accept radial loads up to 140 pounds without encountering this condition. Since the maximum radial load is 77 pounds based on pessimistic assumptions, ample design margin is provided to prevent wiping.

The roller bearing is subject to smaller radial loads than the ball bearing, since the influence of a maldistribution of oil in the separator is very small at this location. The predicted life of the roller bearing is very large over extensive range loads, as indicated in Figure 10. The selected design characteristics of the roller bearing are:

| | |
|---|---|
| Bearing Type | Cylindrical roller bearing |
| Oiling System | Axial cooling slots on bore of inner ring |
| Bearing Size | 55mm bore diameter<br>80mm outer diameter<br>13mm wide |
| Internal Geometry | 24 rollers of 6mm diameter and 7mm length<br>2.70 pitch diameter |

Consumable-electrode vacuum melted M-50 tool steel was selected for the rollers and rings.

In the first quarterly report, preliminary evaluation of the rotor critical speeds was presented as a function of bearing stiffness. The stiffness of the roller bearing is estimated to be 1,400,000 lbs per inch, while the stiffness of the ball bearing is predicted to be 240,000 lbs per inch. The critical speeds of the final rotor configuration were reanalyzed and the results are represented in Figure 11. Two sets of curves are presented in this figure which represent two possible alternatives in the design of the separator. Since the density of the metallic gauze in the separator will be based on experimental results, a pessimistic (heavy) separator is represented in Figure 11, as well as a separator consistent with the

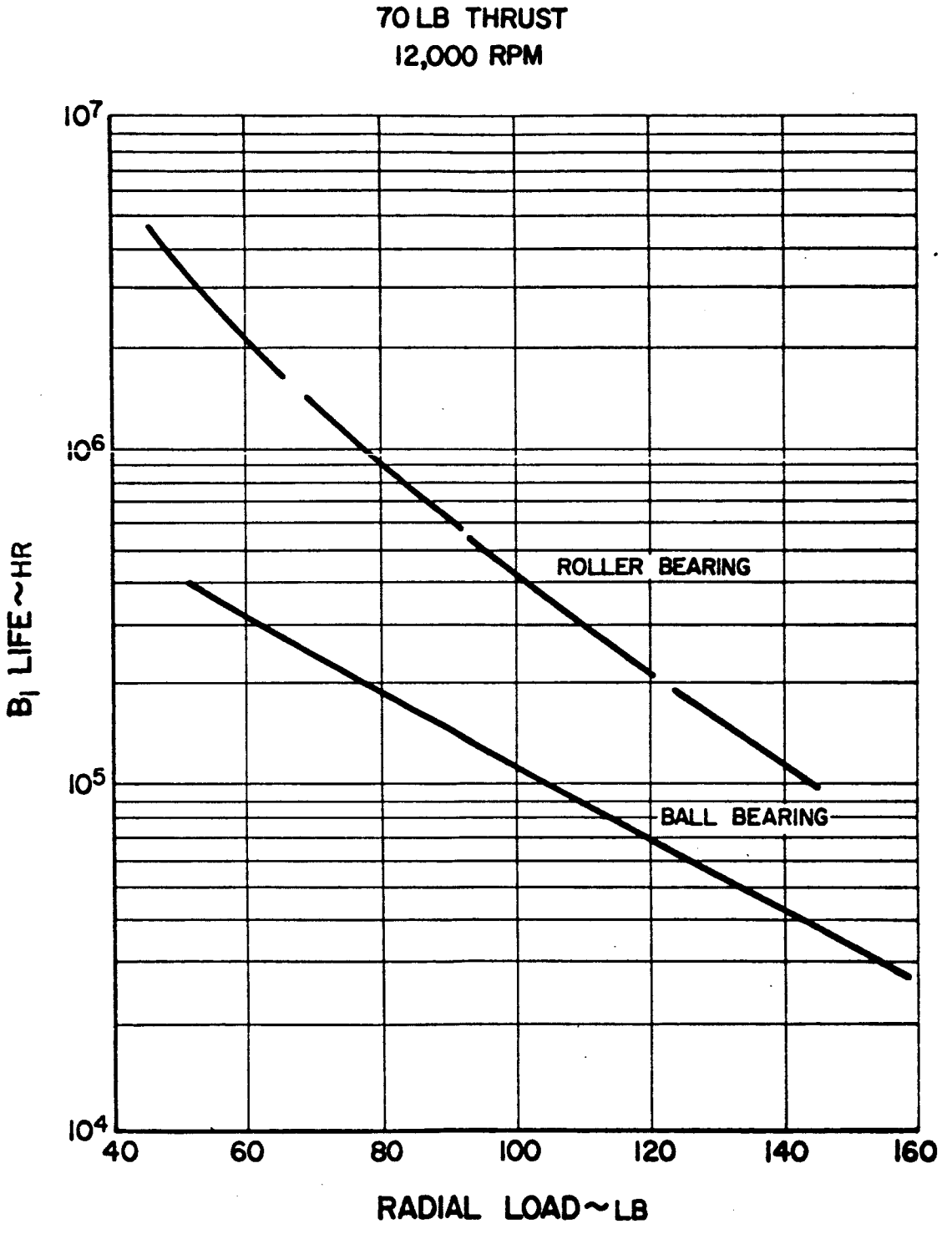


Figure 10 $B_1$ Life vs Radial Load for Turboalternator Bearings

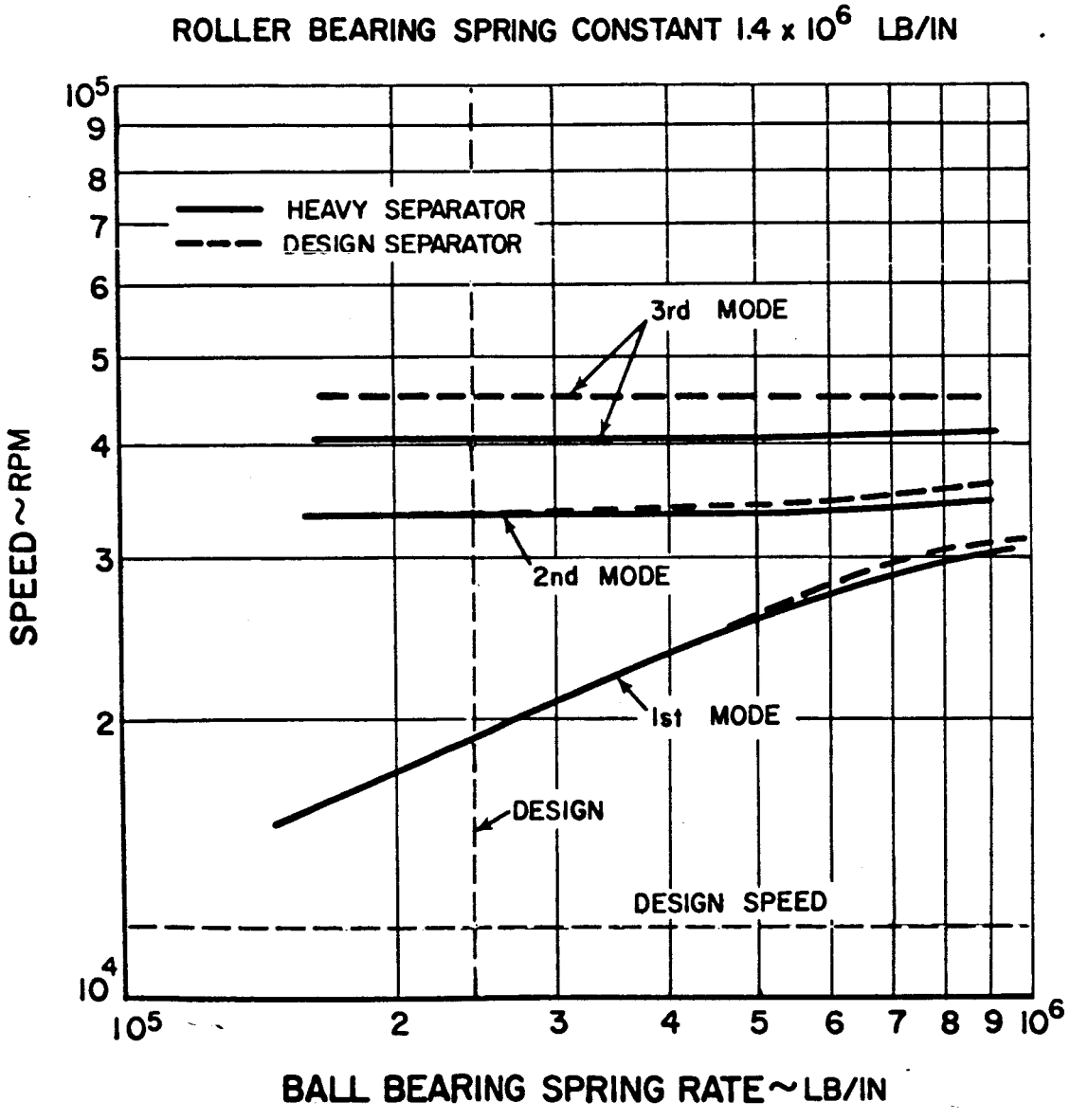


Figure 11 Turboalternator Critical Speeds

anticipated configuration. The turboalternator has a rigid-body critical speed at 19,000 rpm and bent-shaft critical speeds at 33,800 and 40,800 rpm, if the pessimistic separator weight is used. If the normal separator weight is employed, the third critical speed is raised to 45,200 rpm. There are no critical speeds in the range of the operating speed or in the range of the equivalent electrical speed for this machine.

# V. BEARING-SEAL-SCAVENGE RIG

The performance of selected components of the oil-lubricated rolling-element bearing system will be evaluated experimentally. Turbine-compressor components were selected for experimental evaluation because they were considered to be more critical than similar elements in the turboalternator. Since the turbine-compressor bearings, seals, and scavenge pumps are about the same size and located adjacent to each other, one basic test rig was planned in order to test each component separately or in combination. Two versions of the bearing-seal-scavenge test rig have been designed: a seal test rig and a bearing-scavenge rig. The bearing-scavenge rig can also incorporate a seal for certain tests.

During the previous report period, the design of the two versions of the bearing-seal-scavenge rig were nearly completed[2]. During this report period, the designs were completed and detail manufacturing drawings were prepared. Raw material was obtained and fabrication of the rig parts was initiated.

The seal test rig design is presented in Figure 12. The shaft is driven by an air turbine (not shown in Figure 12) and the central portion of the rig contains jet oil lubricated bearings which support the shaft. The test seal is mounted on the outboard end of the shaft. In the turbine-compressor design, Figure 2, the seal is mounted inboard of the bearing and the oil is introduced in the end of the shaft. If this arrangement were used in the seal rig, a second shaft seal between the test rig bearings and the test seal would be required and leakage past the second seal would confuse the evaluation of the seal being tested. Therefore, the arrangement shown in Figure 12 was chosen to provide a dead-end leakage cavity. Since the only source of oil in the cavity is leakage past the test seal, the performance of the test seal can be accurately assessed.

In order to cool the seal, oil is introduced in the turbine drive end of the shaft. In the design reported previously[2], this cooling oil passed through two passages to the test seal area. During this report period, the fabrication of the original seal rig shaft design was found to be uneconomical. Therefore, the shaft was redesigned to provide an annular cooling oil passage rather than the holes employed previously. The revised shaft design is shown in Figure 12.

The bearing-scavenge rig design is presented in Figure 13. This design is a duplicate of the arrangement at one end of the turbine-compressor. Oil and oil-argon mist are introduced at the free end of the shaft and pass

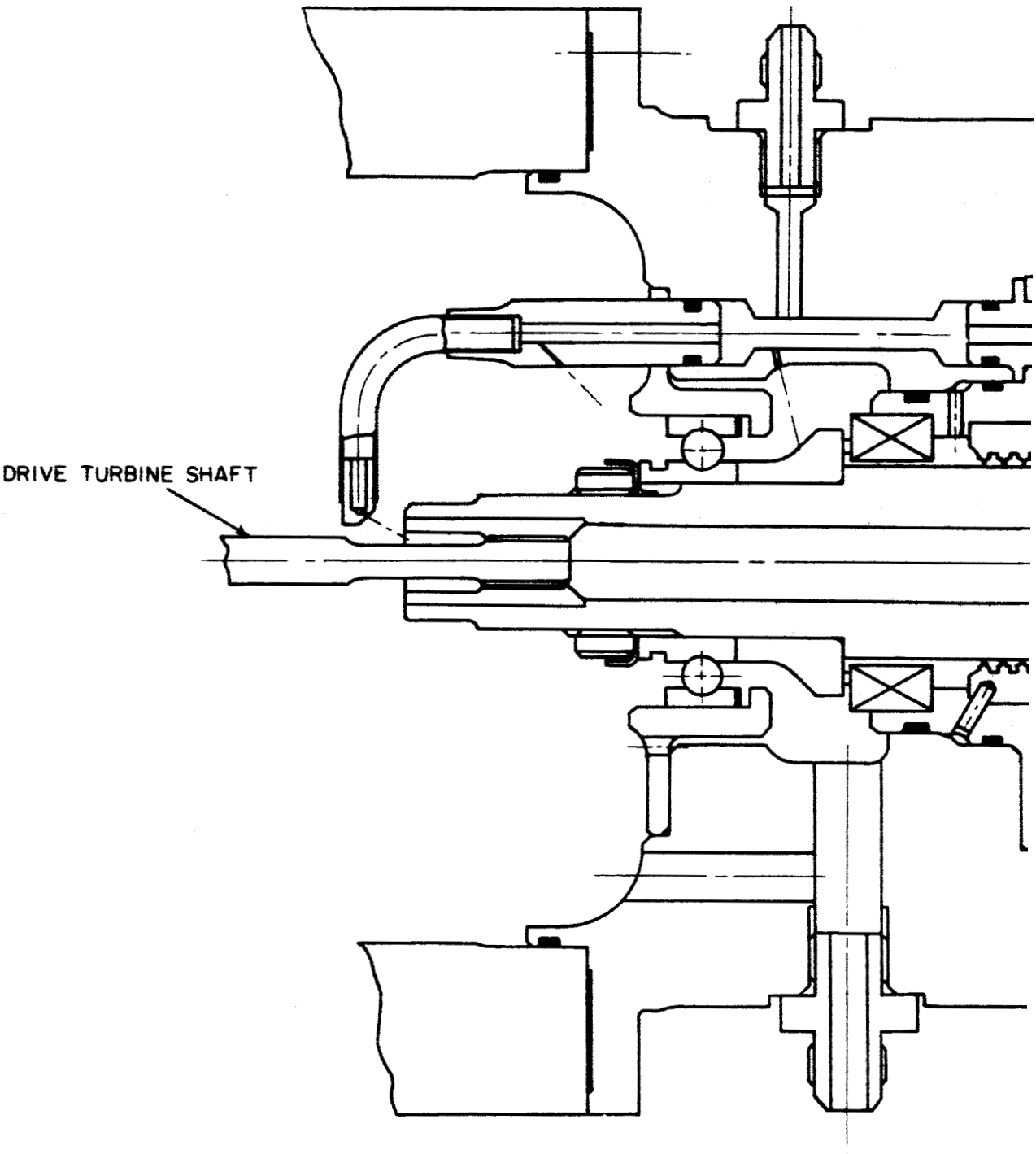


Figure 12 Turbine-Compressor Seal Test Rig

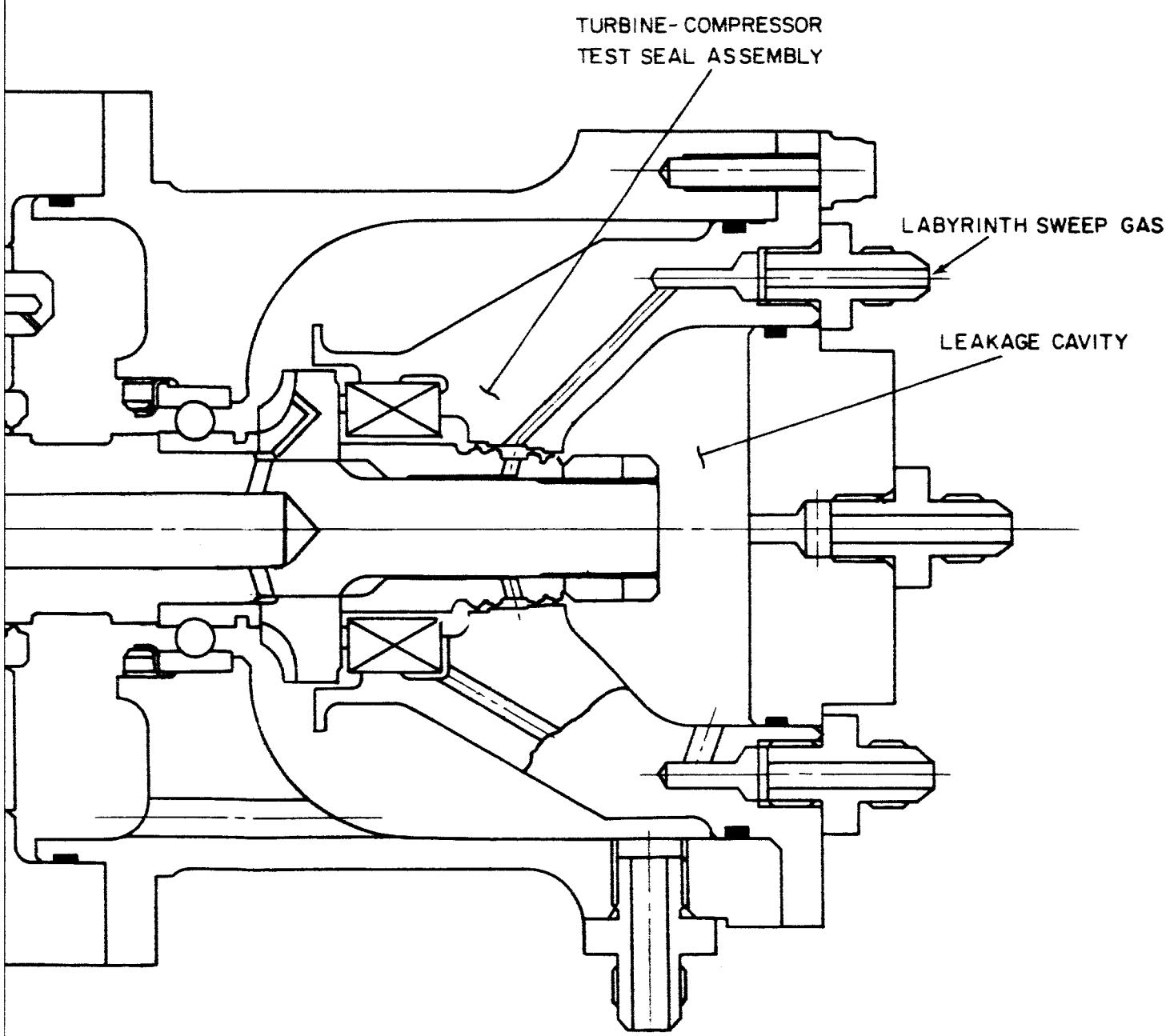
TURBINE- COMPRESSOR
TEST SEAL ASSEMBLY
LABYRINTH SWEEP GAS
LEAKAGE CAVITY

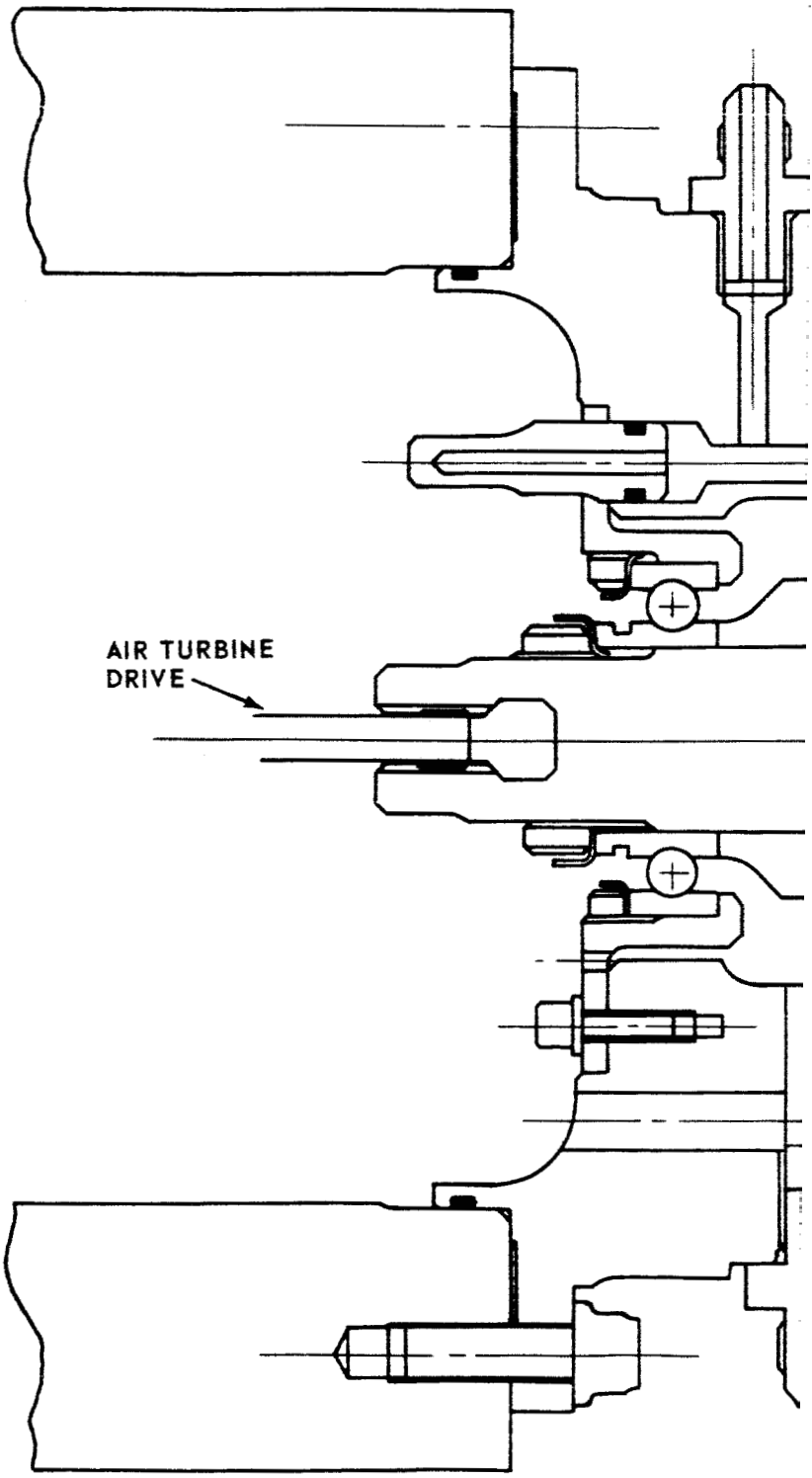


Figure 13 Turbine-Compressor Bearing-Sc

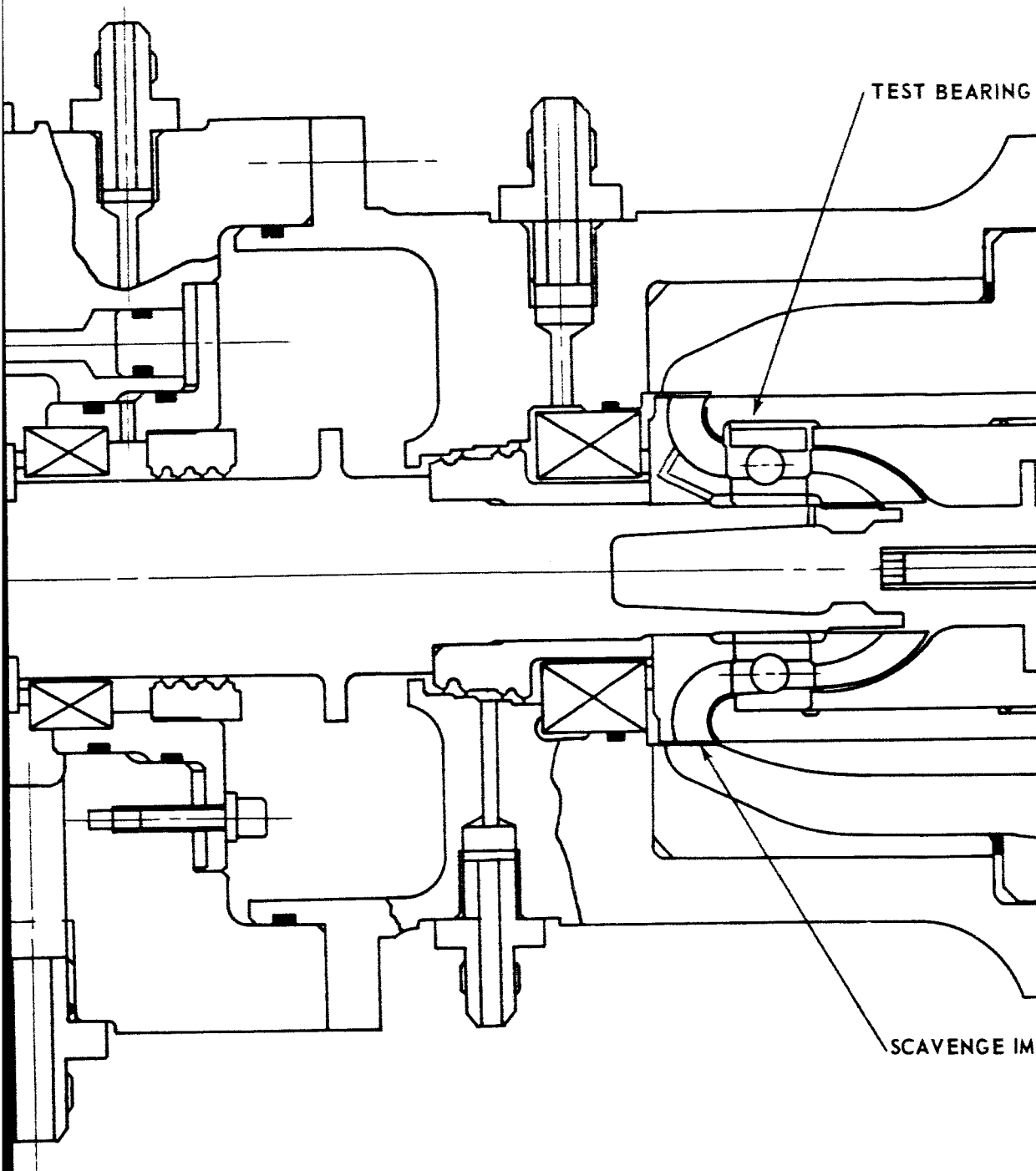


avenge Rig

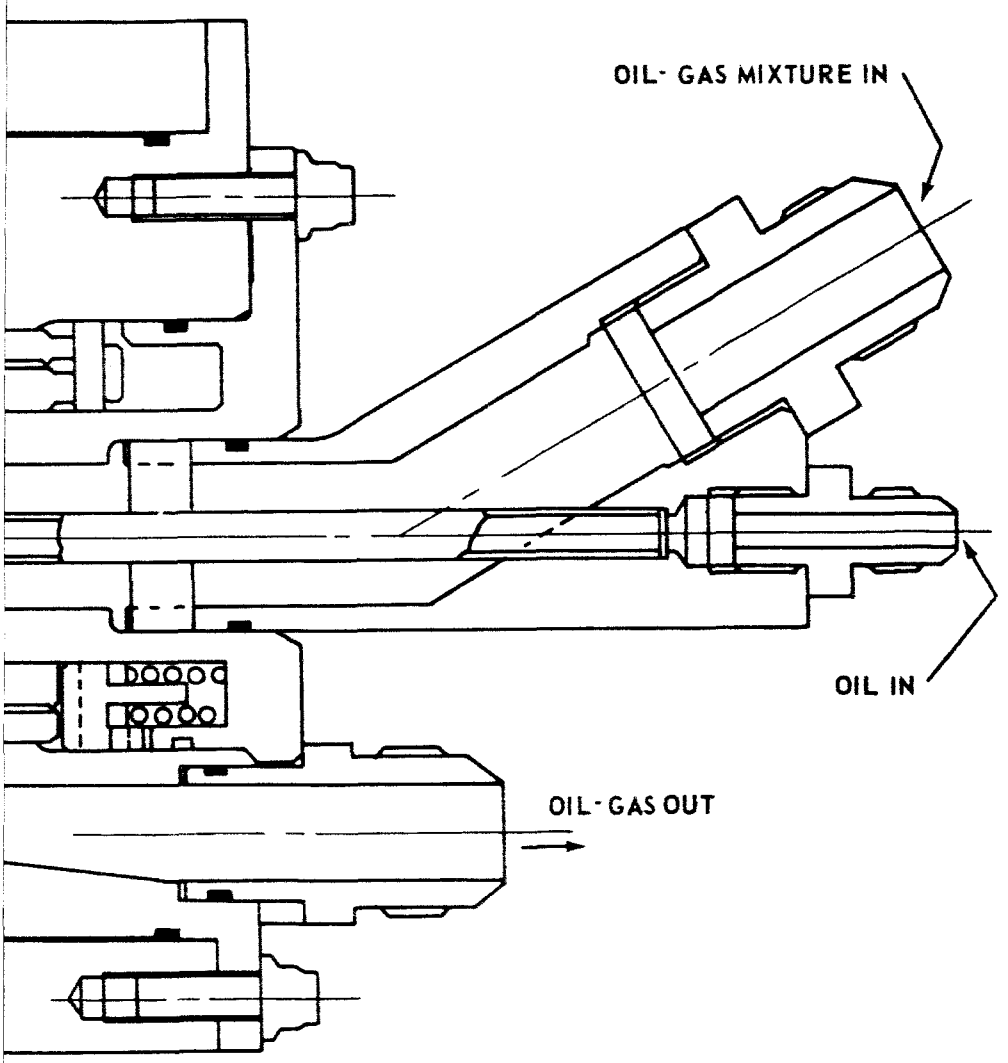


PELLER

through the bearing and scavenge pump in the same way as in the turbine-compressor. The seal can be included in this arrangement if desired. The housing on the test end of the rig and the shaft are, of necessity, not the same as the corresponding part of the seal version of the rig. The drive turbine and rig bearing area employ the same parts as are used in the seal rig.

# VI. SEPARATOR-PUMP RIG

The oil-gas separator and oil pump are two components, in addition to the turbine-compressor bearing, seal, and scavenge components, which have been selected for experimental investigation. Both components are mounted on the free end of the turboalternator and operate at 12,000 rpm.

The separator-pump test rig has been designed to evaluate pump performance, separator performance, and combined pump-separator performance. The general arrangement of the separator-pump test rig, presented in Figure 14, is similar to that of the bearing, seal, and scavenge test rigs. The rig is driven by an air turbine and the test components are overhung from an intermediate housing. The rig configuration presented in Figure 14 combines a scoop pump and a separator section. Initial separation will be accomplished at the scoop pump where the bearing compartment scavenge gas-oil mixture is introduced, filling the shaft reservoir with oil. Oil is pumped from the shaft reservoir to the accumulator by the scoop pump and the gas, oil vapor and overflow oil flow into the separator. In the separator the oil and gas are separated by centrifugal forces. The separated oil is pumped along the sloping outer wall and discharged forward towards the bearing compartment, while the argon is discharged from the rear of the separator and is piped out of the compartment. The test rig is designed to evaluate pump and separator designs individually as well as simultaneously.

During the previous report period, the basic arrangement of the separator-pump rig was developed and the critical speeds were evaluated[2]. During this report period, the design was completed and detail manufacturing drawings were produced. Raw material for the rig parts was procured. The procurement process was started for the rig parts.

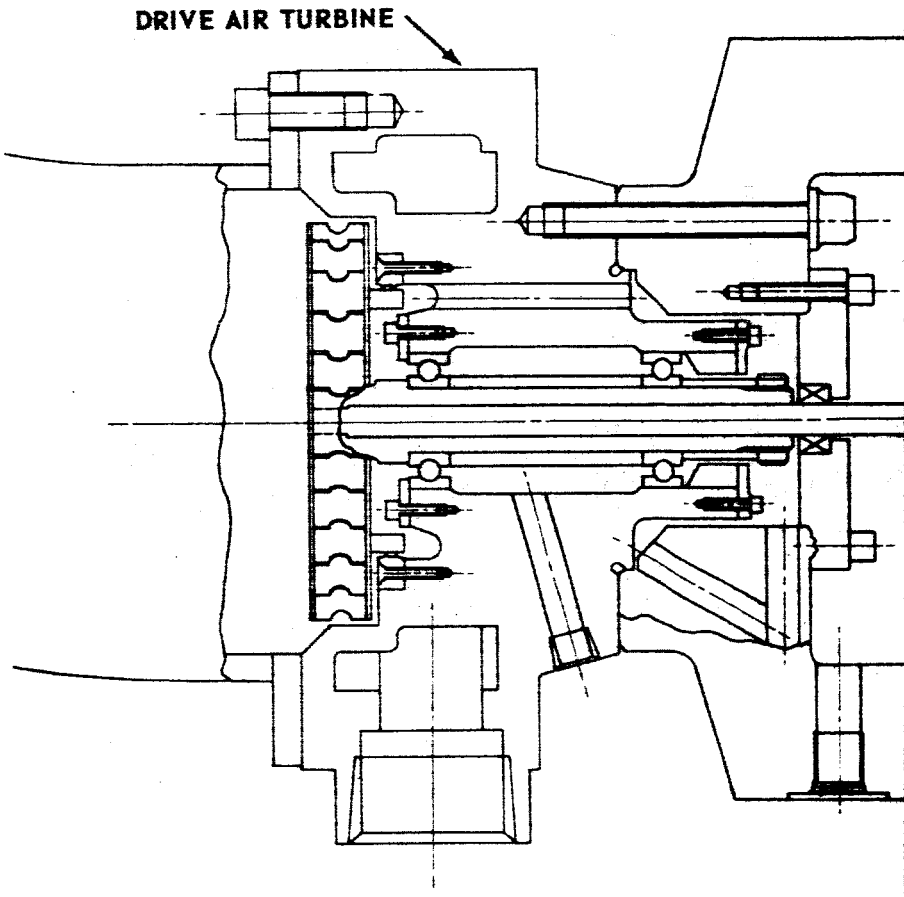


Figure 14 Turboalternator Pump-Sepa

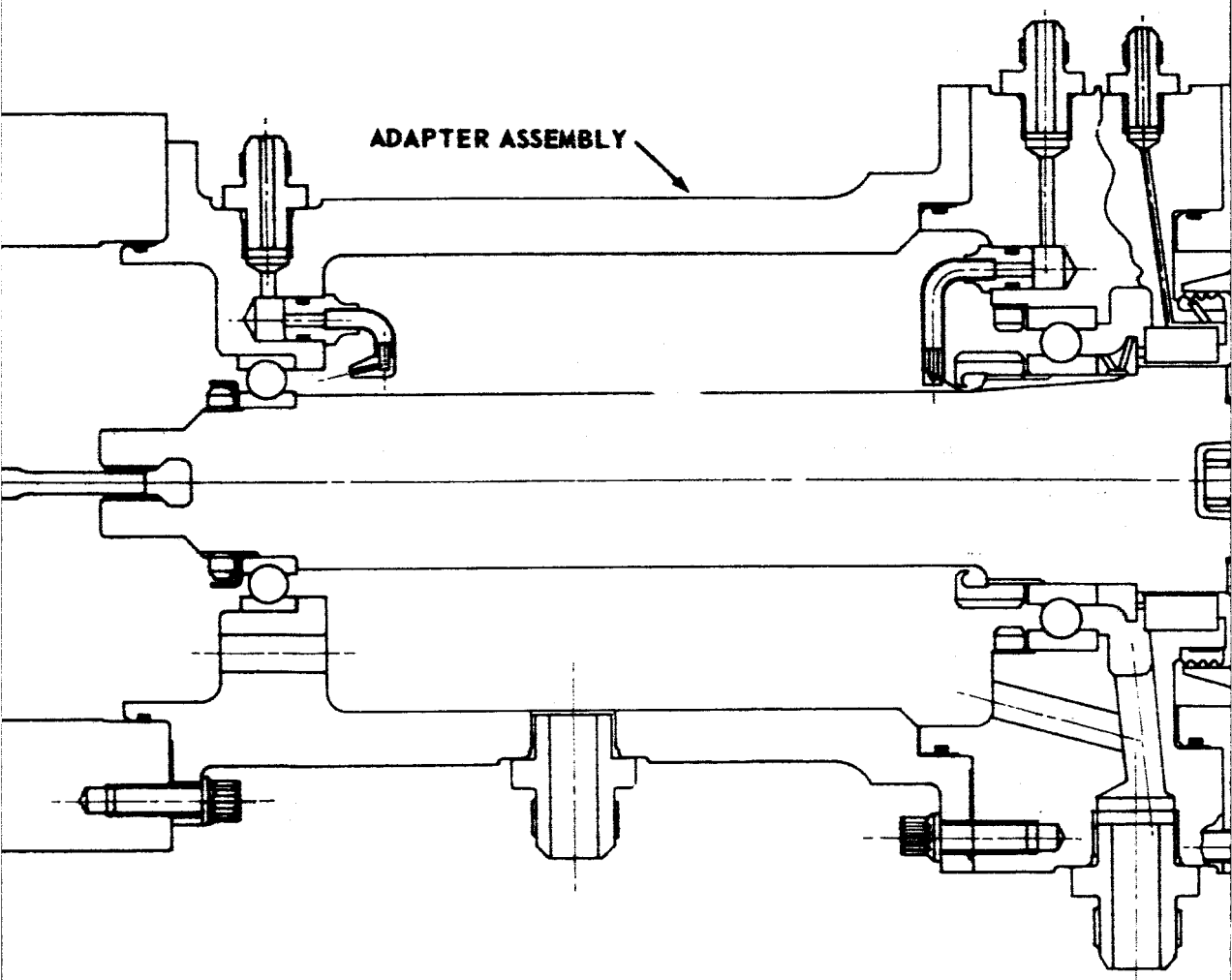


rator Rig

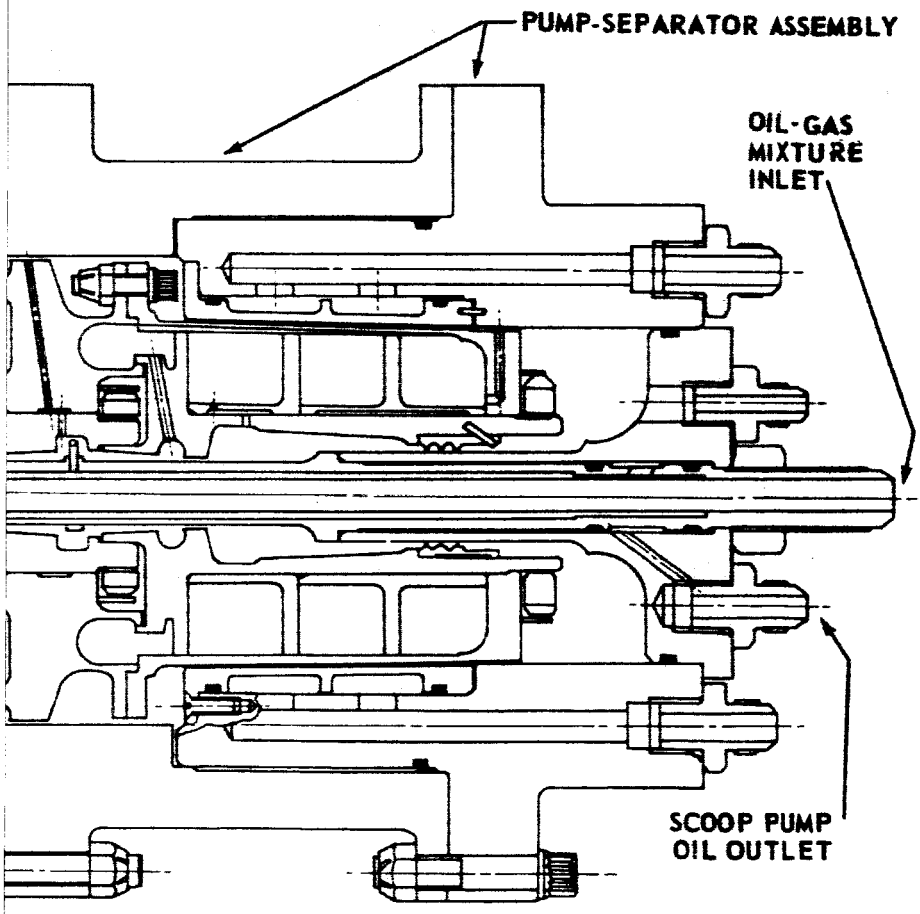
PUMP-SEPARATOR ASSEMBLY
OIL-GAS MIXTURE INLET
SCOOP PUMP OIL OUTLET

# VII. ADSORBER PROGRAM

The lubricant for the rolling-element bearings must be segregated from the high-purity main Brayton-cycle argon system. The design concept being pursued under this contract utilizes a combination of face seals and labyrinth seals to accomplish this separation. Some argon leaks through the face seals into the bearing compartments and this bleed argon must be returned to the main cycle. To prevent contamination of the primary cycle gas, the returning leakage gas must be purified. Oil in the form of droplets will be removed from the gas in a centrifugal separator which will also cool the gas to reduce the oil vapor partial pressure. Final purification of the argon will be accomplished by passing the gas through an adsorber bed prior to returning it to the main cycle at the compressor inlet. Primary emphasis is being placed on the use of molecular sieve materials in the adsorber bed for removal of lubricant from argon. The molecular sieve materials are alkali metal aluminosilicates which have been conditioned by removal of the water of hydration.

As reported previously [1,2] an adsorber test rig has been designed and constructed to evaluate molecular sieve materials for this application. The test rig consists of a vaporizer, a swirl separator, and an adsorber column. Argon is bubbled through heated oil in the vaporizer to produce a mixture containing argon, oil vapor, and entrained oil. The gas-oil mixture leaving the separator is cooled to 100°F, corresponding to system adsorber inlet design temperature. This cooling causes precipitation of finely-divided oil particles in the gas stream which remain suspended in the stream. The gas stream is passed through a swirl separator prior to entering the adsorber test section to remove entrained oil droplets. This separator simulates the function of the centrifugal separator attached to the turboalternator. After leaving the separator, the gas stream which contains some oil passes through the adsorber column. The configuration of the test rig is shown in Figure 15. The tubing connecting the vaporizer to the adsorber column as well as the adsorber column are wrapped with electrical resistance tape to provide the heat necessary for temperature control of these components.

Adsorption evaluation tests of Linde 4A and 13X molecular sieve materials have been made. The previous report[2] presented the results of tests of these two materials in powder form having particle size corresponding to 60-80 mesh. A third test has been conducted using approximately 40 grams of 1/16-inch diameter Linde 13X molecular sieve pellets in the adsorber column. The 13X pellets were conditioned at 300°C for 15 hours

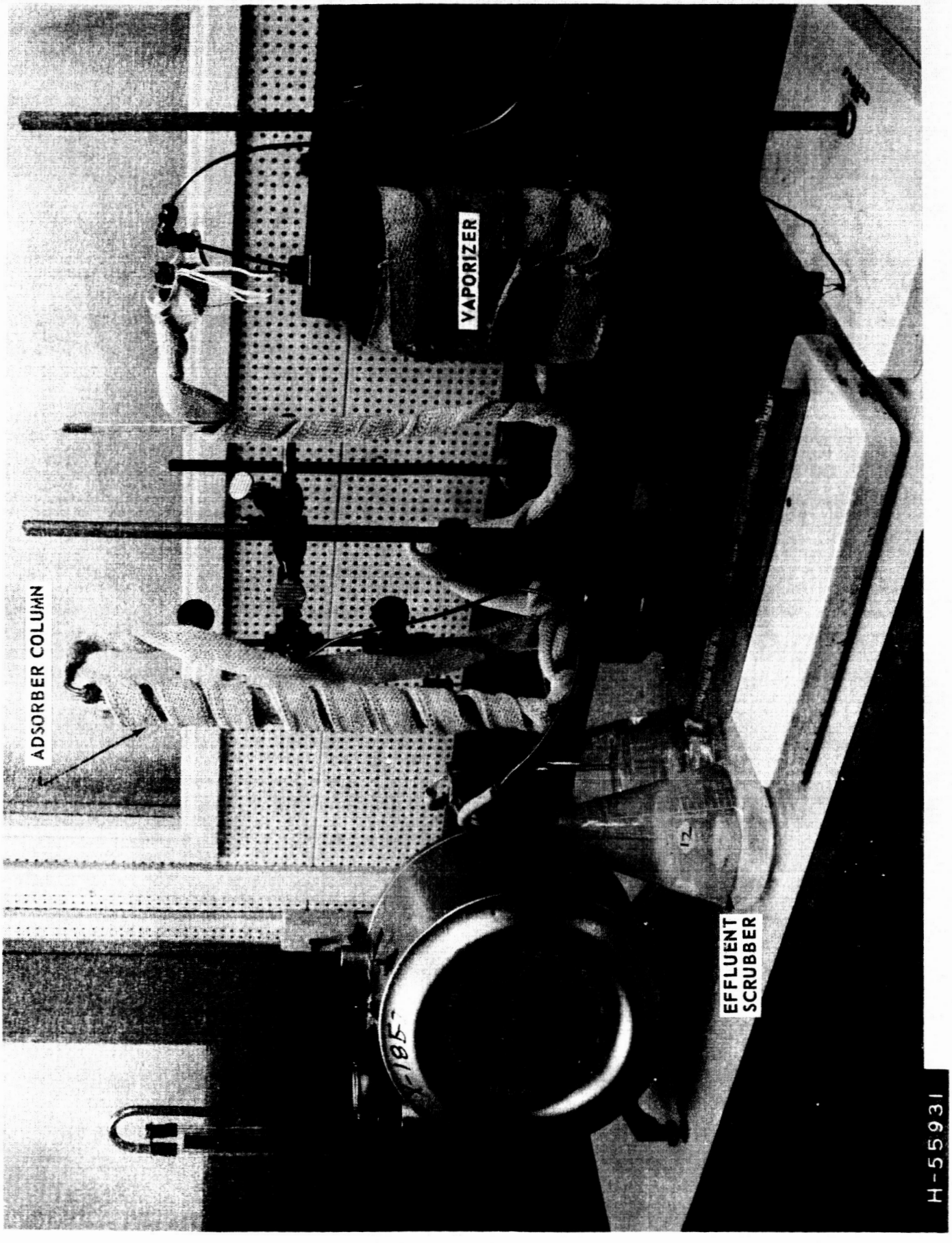


Figure 15 Modified Test Apparatus for Adsorbate Evaluation

prior to the start of the test. The test rig vaporizer was charged with PWA-524 5-ring polyphenyl ether oil and was operated at 350°F. The adsorber bed column was maintained at 100°F during the test which was operated for a period of 100 hours at an argon flow rate of approximately 1 liter per minute. The results of the analysis of the oil distribution for the adsorber material in this test is as follows:

| Portion of Column | Grams of Oil Adsorbed | Micrograms of Oil per Gram of Argon |
|---|---|---|
| first 1/8 | 0.238 | 21 |
| second 1/8 | 0.029 | 2.6 |
| third 1/8 | 0.008 | 0.71 |
| fourth 1/8 | less than 0.0004 | less than 0.04 |
| cumulative fifth through eighth | less than 0.0004 | less than 0.04 |

A test was conducted to determine the saturation capability of the 1/16-inch diameter 13X molecular sieve pellets for adsorption of PWA-524 five-ring polyphenyl ether oil. A weighed quantity of the 13X pellets were soaked in PWA-524 oil and subsequently desiccated at 200°F over wire screen and filter paper for 50 hours. The weight of oil adsorbed per gram of 13X molecular sieve pellet material in this test was determined to be 0.3305 gm.

In the rolling-element bearing lubrication system discussed in the second quarterly report, the pressure drop across the adsorber bed determines the argon pressure in the bearing compartments, which determines the pressure difference across the face seals. In order to minimize oil weepage through the face seals, a high pressure difference should be maintained which requires a low pressure drop across the adsorber. Therefore, tests were conducted to determine the pressure drop with various adsorber configurations. Adsorber columns were fabricated with static taps located 10 inches apart near the inlet and discharge of the column. Three adsorber columns were constructed with inside diameters of 0.41, 0.87 and 1.34 inch. A photograph of one adsorber column setup for pressure drop tests is shown in Figure 16. The pressure drop results using this apparatus with an argon flow rate of 1 liter per minute are:

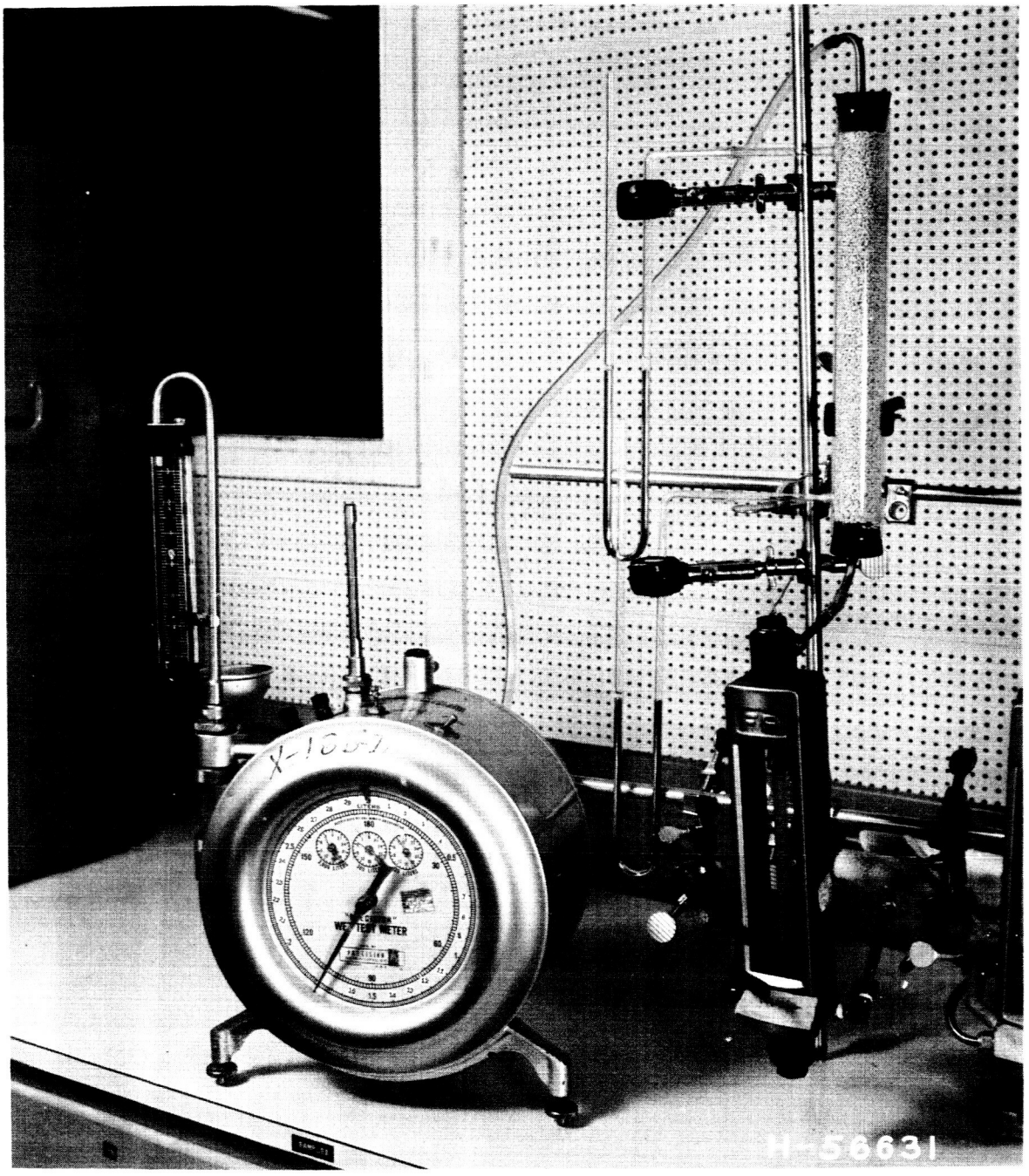


Figure 16 Pressure Drop Test Rig

| Tube No. | Inside Diameter of Tube, Inch | Molecular Sieve Form | Pressure Drop, psi |
|---|---|---|---|
| 1 | 0.41 | 1/16-inch dia. 13X pellets | 0.018 |
| 2 | 0.87 | 1/16-inch dia. 13X pellets | 0.010 |
| 3 | 1.34 | 1/16-inch dia. 13X pellets | 0.001 |
| 1 | 0.41 | 60-80 mesh 13X power | 1.5 |

No unusual phenomena were observed during these tests. Evidently the pellet form of the adsorber material provides much lower pressure drops than the powder form.

Since the Linde 13X material in pellet form provides satisfactory adsorption characteristics and offers a significant pressure drop advantage, this material was selected for the 1000-hour adsorber test. The test rig configuration for the 1,000-hour adsorber endurance test was designed and the necessary apparatus was fabricated and assembled. The diameter of the adsorber column for this test was increased over that of the 100-hour test rig column to provide a ratio of minimum bed diameter to pellet diameter of 20 to 1. A Pyrex tube having a 1.31 inch inside diameter was selected for the adsorber bed container. The length of the column was also increased over that of the 100-hour test column to approximately 33 inches. Pressure taps have been provided at the inlet, midpoint, and discharge of the bed so that pressure drop measurements across the bed can be made during the 1,000-hour test. The design flow of argon through the bed corresponds to the mass flow rate per unit cross-sectional area that was used in the 100-hour adsorber tests. Dual manifold vaporizer and swirl separators have been incorporated into the 1,000-hour adsorber endurance test rig so that these units can be serviced without interrupting the test. In addition, the size of the swirl separator was increased to accommodate the increased argon flow rate. A total hydrocarbon analyzer has been incorporated in the endurance test rig to monitor the argon flow for oil content leaving the adsorber bed. This analyzer will be used periodically to determine if any oil is being discharged from the adsorber. The argon leaving the adsorber column flows through a trap intended to collect all of the oil leaving the bed. At the end of the 1000-hour test the contents of the trap will be measured to determine the total quantity of oil which has been discharged from the adsorber. A photograph of the 1000-hour adsorber endurance test rig is presented in Figure 17.

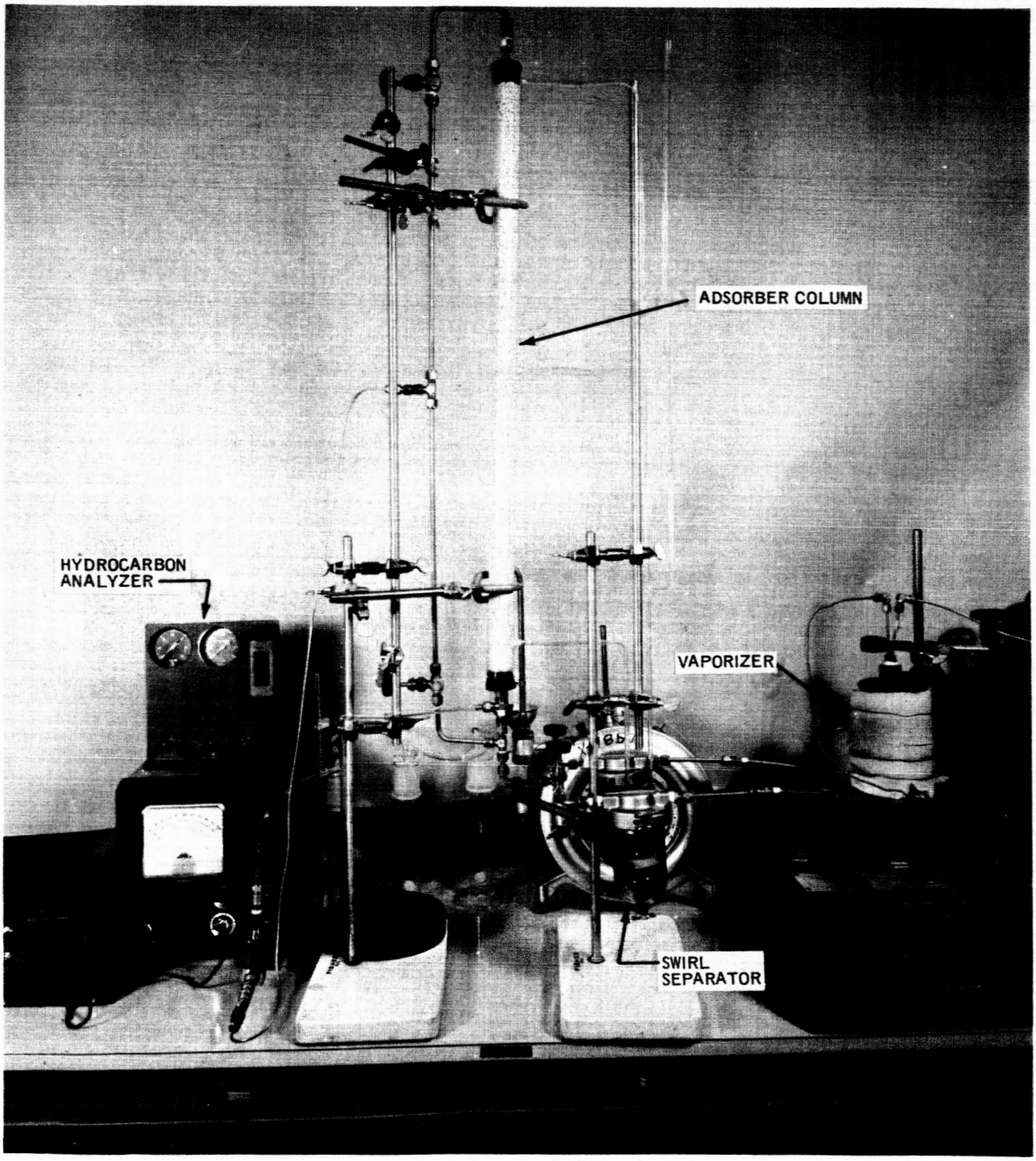


Figure 17 Adsorber Apparatus for 1000-Hour Endurance Test H-57706

# APPENDIX 1

## References

# APPENDIX 1
## References

1. First Quarterly Progress Report, Brayton-Cycle Turbomachinery Rolling-Element Bearing System, NASA CR-54785, PWA-2713, October 1965

2. Second Quarterly Progress Report, Brayton-Cycle Turbomachinery Rolling-Element Bearing System, NASA CR-54915, PWA-2780, February 1966

# APPENDIX 2

## Basic Relations for an Annular Jet Scavenge Pump

# APPENDIX 2

## Basic Relations for an Annular Jet Scavenge Pump

The jet scavenge pump basically consists of a passage in which high velocity liquid is centrally injected and low velocity gas enters on each side of the liquid. This type of pump is represented in a simplified schematic in Figure 18. In the actual pump, the liquid is shed from a rotating impeller and enters a radial passage. The radial velocity of the liquid is very low but the tangential velocity is essentially the wheel speed of the impeller, which is about 400 to 500 feet per second. A representative liquid velocity vector diagram at the entrance to the throat of the pump is shown in Figure 19. The schematic diagram of the pump, Figure 18, is a representation in the liquid flow direction which is nearly tangential. The liquid enters the passage at high velocity and the gas enters at low velocity. After some distance, the shear between the liquid and the gas reduces the liquid velocity to essentially the same velocity as the gas. Since the gas is flowing in the equivalent of a duct of nearly constant area, and since the liquid occupies a very small portion of the volume, the bulk of the energy transferred from the liquid to the gas produces a static pressure rise in the gas.

The pertinent assumptions made in the following analysis are:

1) identical pressures and temperatures exist for the two phases at a given section of flow,
2) the gas phase is insoluble in the liquid phase,
3) isothermal conditions,
4) argon gas conforms to the ideal gas law, and
5) the losses incurred from oil discharge to the constant-area throat entrance are negligible.

### Design Equations

At any point in the mixing section of a small section of length dx from the actuating and the entrained jet, the velocities change by $dc_1$ and $dc_2$, and the pressure by dp. The application of the momentum equation to the actuating and then to the entrained jet gives

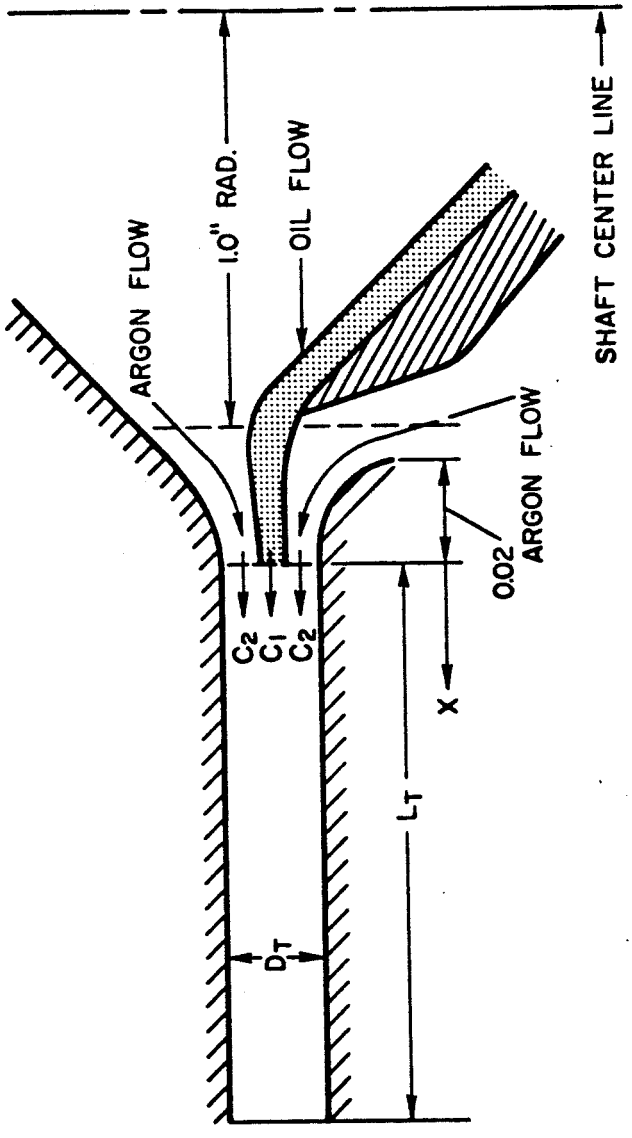


Figure 18 Schematic of Annular Jet Scavenge Pump

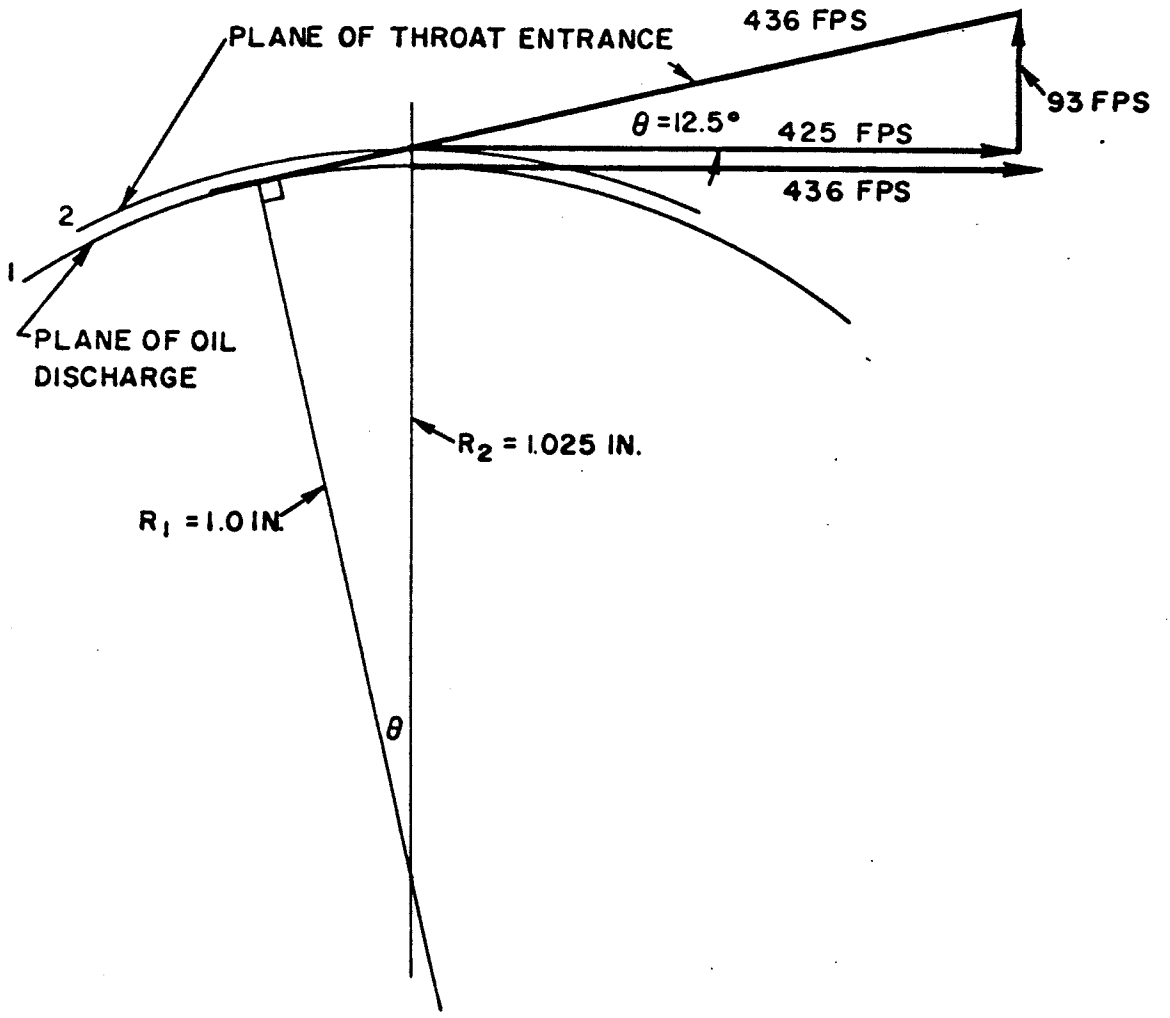


Figure 19 Representative Velocity Triangle for Annular Jet Scavenge Pump

$$\frac{w_1}{g_c} dc_1 + A_L\, dp + dF_i = 0 \qquad (1)$$

$$\frac{w_2}{g_c} dc_2 + (A_t - A_L)\, dp - dF_i + dF_w = 0 \qquad (2)$$

where $dF_i$ = effective drag force at the interface
$dF_w$ = force due to inner wall friction

The effective drag force in a small element $Z_i dx$ of the boundary surface between actuating and entrained jet is

$$dP = \tau Z_i dx \qquad (3)$$

where $\tau$ = apparent shearing stress
$Z_i$ = interface wetted perimeter

For two dissimilar fluids the apparent shearing stress is defined as follows:

$$\tau = \frac{2\chi}{2 + \sqrt{\rho_1/\rho_2} + \sqrt{\rho_2/\rho_1}} \frac{c_1 \rho_1 - c_2 \rho_2}{g_c} (c_1 - c_2)$$

The force due to inner wall friction is represented by the equation

$$dF_w = \lambda \frac{\rho_2}{2 g_c} c_2^2 Z_w dx \qquad (4)$$

where $Z_w$ = wetted perimeter of mixing section

The cross-section of the mixing throat is taken to be rectangular. Combining Equations (1) and (2) with the above definitions of $dF_i$ and $dF_w$ gives for the change in velocity with respect to throat distance

$$\frac{dc_1}{dx} = \frac{K_1 - K_2}{\frac{\rho_1 c_1}{g_c}\left[1 - \frac{\rho_2}{\rho_1}(RC)^2\left(1 - \frac{bc_1}{a}(RC)\right)\right]} \qquad (5)$$

where $a = w_2 \rho_1$

$b = A_L \rho_2 \rho_1 / 144$

$(RC) = a/(bc_1 - k)$

$k = w_1 \rho_2$

$$K_1 = \frac{\lambda M \rho_2 \rho_1}{144 g_c (A_t \rho_1 c_1/144 - w_1)} c_1^3 (RC)^2$$

$$K_2 = \frac{B}{6 g_c} c_1^3 \left(\frac{\rho_1}{w_1} \frac{\rho_2}{w_2} (RC)\right)\left(1 - (RC)\right)\left(\rho_1 - \rho_2 (RC)\right)\frac{M}{12}$$

$$B = \frac{2\chi}{2 + \sqrt{\rho_1/\rho_2} + \sqrt{\rho_2/\rho_1}}$$

The pressure rise in the throat is given by the equation

$$\Delta p = \frac{w_1}{g_c A_t} (c_{10} - c_1) - \frac{w_2}{g_c A_t} (c_2 - c_{20}) - \frac{\lambda}{144} \frac{M}{A_t} \frac{\rho_2}{g_c} c_{20} c_2 x \quad (6)$$

where $c_2 = \frac{ac_1}{bc_1 - k}$

Equation (5) can be solved numerically using the Runge-Kutta-Gill[1] system for solution of a first-order differential equation. The pressure rise in the throat can then be readily obtained from Equation (6).

Discussion

The basis for the equations given above was NACA Technical Memo No. 982[2]. However, the work here has modified the equations to allow for the 2 component-2 phase flow system.

The effective dragging force in Equation (3) is a function of the friction coefficient between two moving fluid layers, $\chi$. This coefficient significantly affects the results. Therefore, it is desirable to be able to determine the value of $\chi$ as accurately as possible.

[1] Gill, S., Proceedings of Cambridge Philosophical Society, Volume 47, p. 96, 1951

[2] Flugel, G., NACA Technical Memo No. 982, July 1941

Flugel stated that $\chi$, according to recent findings (circa 1939), averages 0.10. In his development he assumes $\chi$ to be constant. However, he admits that it actually varies. Schlichting[1] comments on the variation of a correlation coefficient (similar to $\chi$) as a function of radial distance in the throat. Due to the expansion of the primary fluid in the throat, $\chi$ also varies as a function of throat length. If reliable experimental data exist, a correlation between $\chi$ and throat distance can be devised (this has been done for a liquid-liquid system with satisfactory results).

For lack of any experimental data, $\chi$ for the present development has been taken to be constant. For the range of $\chi$'s tested, the maximum pressure rise is affected only slightly, however, the corresponding throat length is significantly changed. The following table is representative of the sensitivity of pump performance to the magnitude of $c_2/c_1$ for a typical pump geometry and operating condition

| $\chi$ | Pressure Rise $(\Delta P_t)$ max | Throat Length $L_t$ | Velocity Ratio $c_2/c_1$ |
|---|---|---|---|
| 0.02 | 5.2698 | 0.432 | 0.9929 |
| 0.10 | 5.2930 | 0.180 | 0.9993 |
| 0.20 | 5.2963 | 0.108 | 0.9995 |

For the design of the jet scavenge pump a conservative value of $\chi = 0.02$ was selected. As a result, the design throat length may be longer than necessary to accomplish full pressure rise. However, the increase in friction pressure loss that may result is small.

[1] Schlicting, H., Boundary Layer Theory, McGraw-Hill Book Co., New York, 1960, p. 466

## NOMENCLATURE

| Symbol | Definition | Units |
|---|---|---|
| A | cross-sectional area | $in^2$ |
| c | velocity | ft/sec |
| F | force | lb |
| $g_c$ | acceleration of gravity | $lb_m ft/lb_f sec^2$ |
| M | circumferential length | in. |
| L | length | in. |
| n | dimensionless flow ratio | - |
| $\Delta p$ | pressure rise | psi |
| R | dimensionless area ratio | - |
| w | weight of fluid per second | lb/sec |
| x | length | in. |
| Z | wetted perimeter | in. |
| $\lambda$ | skin friction factor | - |
| $\rho$ | density | $lb_m/ft^3$ |
| $\tau$ | shear stress | $lb/in^2$ |
| X | interfacial friction factor | - |

| Subscripts | Definition |
|---|---|
| i | interface |
| L | liquid |
| t | constant-area throat |
| w | wall |
| o | throat entrance |
| 1 | actuating (oil) jet |
| 2 | entrained (argon) jet |

# Distribution List
# Contract NAS3-7635

| To | No. of Copies |
|---|---|
| **National Aeronautics and Space Administration** | |
| **Lewis Research Center** | |
| 21000 Brookpark Road | |
| Cleveland, Ohio 44135 | |
| Attention: B. Lubarsky, MS 500-201 | 1 |
| I. Pinkel, MS 5-3 | 1 |
| D. G. Beremand, MS 500-201 | 1 |
| J. Heller, MS 500-201 | 1 |
| W. Stewart, MS 5-9 | 1 |
| D. C. Guentert, MS 500-201 | 1 |
| J. E. Dilley, MS 500-309 | 1 |
| W. J. Anderson, MS 6-1 | 1 |
| Z. Nemeth, MS 6-1 | 1 |
| E. Zaretsky, MS 49-1 | 1 |
| R. L. Johnson, MS 5-8 | 1 |
| L. P. Ludwig, MS 5-8 | 1 |
| H. Rohlik, MS 6-1 | 1 |
| B. Wong, MS 6-1 | 1 |
| A. Straquadine, MS 500-203 | 1 |
| E. Bisson, MS 5-3 | 1 |
| L. Gertsma, MS 500-202 | 1 |
| D. T. Bernatowicz, MS 500-201 | 1 |
| T. A. Moss, MS 500-201 | 1 |
| F. Dutee, MS 21-4 | 1 |
| L. W. Ream, MS 500-201 | 1 |
| Report Control, MS 5-5 | 1 |
| Technology Utilization Office, MS 3-19 | 1 |
| Librarian | 1 |
| **National Aeronautics and Space Administration** | |
| **Washington, D. C. 20546** | |
| Attention: T. C. Evans, MTF | 1 |
| F. P. Dixon, MTG | 1 |
| A. M. Andrus, ST | 1 |
| H. Rochen, RN | 1 |
| J. J. Lynch, RNP | 1 |
| **National Aeronautics and Space Administration** | |
| **Scientific and Technical Information Facility** | |
| P. O. Box 33, College Park, Maryland 20740 | |
| Attention: Acquisitions Branch, SQT-34054 | 2+ repro |
| **National Aeronautics and Space Administration** | |
| **Goddard Space Flight Center** | |
| Greenbelt, Maryland 20771 | |
| Attention: W. R. Cherry | 1 |
| Librarian | 1 |
| **National Aeronautics and Space Administration** | |
| **Langley Research Center** | |
| Langley Station, Hampton, Virginia 23365 | |
| Attention: R. C. Wells | 1 |
| Librarian | 1 |
| **National Aeronautics and Space Administration** | |
| **George C. Marshall Space Flight Center** | |
| Huntsville, Alabama 35812 | |
| Attention: E. Stuhlinger | 1 |
| Librarian | 1 |
| **National Aeronautics and Space Administration** | |
| **Manned Spacecraft Center** | |
| Houston, Texas 77058 | |
| Attention: R. B. Ferguson | 1 |
| Librarian | 1 |
| **National Aeronautics and Space Administration** | |
| **Jet Propulsion Laboratory** | |
| 4800 Oak Grove Drive | |
| Pasadena, California 91103 | |
| Attention: J. W. Goldsmith | 1 |
| Librarian | 1 |
| **National Aeronautics and Space Administration** | |
| **Ames Research Center** | |
| Moffett Field, California 94035 | |
| Attention: Librarian | 1 |
| **Electronic Research Center** | |
| 575 Technology Square | |
| Cambridge, Massachusetts, 02139 | |
| Attention: Librarian | 1 |

| To: | No. of Copies |
|---|---|
| **U.S. Atomic Energy Commission, DRD** | |
| **Washington, D.C. 20454** | |
| Attention: N. Grossman | 1 |
| J. LaScalzo | 1 |
| R. Oehl | 1 |
| D. B. Hoatson, ARB | 1 |
| Librarian | 1 |
| **U. S. Atomic Energy Commission** | |
| **Technical Information Extension** | |
| P. O. Box 62, Oak Ridge, Tennessee 37831 | |
| Attention: Librarian | 1 |
| **U. S. Atomic Energy Commission** | |
| **Argonne National Laboratory** | |
| 9700 South Cass Avenue | |
| Argonne, Illinois 60440 | |
| Attention: Librarian | 1 |
| **U. S. Army Engineer R&D Laboratories** | |
| **Gas Turbine Test Facility** | |
| Fort Belvoir, Virginia 22060 | |
| Attention: W. Crim | 1 |
| **Department of the Navy** | |
| **Office of Naval Research** | |
| Washington, D. C. 20360 | |
| Attention: Dr. R. Roberts | 1 |
| **Department of the Navy** | |
| **Bureau of Naval Weapons** | |
| Washington 25, D.C. | |
| Attention: Code RAPP | 1 |
| **Department of the Navy** | |
| **Bureau of Ships** | |
| Washington 25, D. C. | |
| Attention: G. L. Graves | 1 |
| **Department of the Navy** | |
| **Naval Research Laboratory** | |
| Washington, D. C. 20390 | |
| Attention: Librarian | 1 |
| **Air Force Systems Command** | |
| **Aeronautical Systems Division** | |
| Wright-Patterson AFB, Ohio 45433 | |
| Attention: G. W. Sherman, APIP | 1 |
| Librarian | 1 |
| **Air Force Aero Propulsion Laboratory** | |
| Wright-Patterson AFB, Ohio 45433 | |
| Attention: John L. Morris, APFL | 1 |
| **National Bureau of Standards** | |
| Washington 25, D. C. | |
| Attention: Librarian | 1 |
| **Massachusetts Institute of Technology** | |
| Cambridge, Massachusetts 02139 | |
| Attention: Librarian | 1 |
| **University of Pennsylvania** | |
| **Power Information Center, Moore School Building** | |
| 200 South 33rd Street | |
| Philadelphia, Pennsulvania 19104 | 1 |
| **Battelle-Northwest** | |
| P. O. Box 999, Richland, Washington 99352 | |
| Attention: Librarian | 1 |
| **Institute for Defense Analyses** | |
| 400 Army Navy Drive | |
| Arlington, Virginia 22202 | |
| Attention: Librarian | 1 |
| **The Franklin Institute** | |
| **Benjamin Franklin Parkway at 20th Street** | |
| **Philadelphia, Pennsylvania 19103** | |
| **Attention: Librarian** | 1 |

| To: | No. of Copies |
|---|---|
| The Rand Corporation<br>1700 Main Street<br>Santa Monica, California<br>Attention: Librarian | 1 |
| Williams Research<br>Walled Lake, Michigan<br>Attention: Librarian | 1 |
| Aerojet-General Coporation<br>Azusa, California 91703<br>Attention: Librarian | 1 |
| Aerojet-General Nucleonics<br>San Ramon, California 94583<br>Attention: Librarian | 1 |
| AiResearch Manufacturing Company<br>A Division of the Garrett Corporation<br>Phoenix, Arizona 85034<br>Attention: Librarian | 1 |
| AiResearch Manufacturing Company<br>A Division of the Garrett Corporation<br>9851 Sepulveda Boulevard<br>Los Angeles, California 90009<br>Attention: Librarian | 1 |
| Avco Rand Corporation<br>201 Lowell Street<br>Wilmington, Massachusetts<br>Attention: Librarian | 1 |
| Barden Corporation<br>Danbury, Connecticut 06810<br>Attention: Technical Library | 1 |
| Chrysler Corporation<br>Space Division, Technical Information Center<br>P. O. Box 26018, New Orleans, Louisiana 70126<br>Attention: Librarian | 1 |
| Douglas Aircraft Company<br>3000 Ocean Park Boulevard<br>Santa Monica, California<br>Attention: Librarian | 1 |
| Electro-Optical Systems, Inc.<br>300 North Halstead Avenue<br>Pasadena, California 91107<br>Attention: Librarian | 1 |
| Fairchild Hiller<br>Republic Aviation Division<br>Farmingdale, Long Island, New York 11735<br>Attention: Librarian | 1 |
| General Dynamics Corporation<br>General Atomic Division<br>San Diego, California<br>Attention: Librarian 92112 | 1 |
| General Electric Company<br>Flight Propulsion Laboratory Department<br>Cincinnati, Ohio 45215<br>Attention: Librarian | 1 |
| General Electric Company<br>Lynn, Massachusetts<br>Attention: Librarian | 1 |
| General Electric Company<br>Missile and Space Vehicle Department<br>3198 Chestnut Street<br>Philadelphia, Pennsylvania 19104<br>Attention: Librarian | 1 |
| Lockheed Aircraft Corporation<br>Missiles & Space Division<br>P. O. Box 504, Sunnyvale, California<br>Attention: Librarian | 1 |

| To: | No. of Copies |
|---|---|
| Martin Company, Baltimore Division<br>Martin-Marietta Corporation<br>P. O. Box 5042, Baltimore, Maryland 21203<br>Attention: Librarian | 1 |
| Mechanical Technology Incorporated<br>968 Albany-Shaker Road<br>Latham, New York 12110<br>Attention: Librarian | 1 |
| North American Aviation, Inc.<br>Atomics International Division<br>8900 DeSoto Avenue<br>Canoga Park, California<br>Attention: Librarian | 1 |
| North American Aviation, Inc.<br>Space and Information Systems Division<br>Downey, California 90241<br>Attention: Librarian | 1 |
| Philco Corporation, Aeronutronic Division<br>Ford Road, Newport Beach, California 92663<br>Attention: Librarian | 1 |
| Solar<br>2200 Pacific Highway<br>San Diego, California 92112<br>Attention: Librarian | 1 |
| Space General Corporation<br>9200 East Flair Drive<br>El Monte, California<br>Attention: Librarian | 1 |
| Space Technology Laboratories, Inc.<br>One Space Park<br>Redondo Beach, California<br>Attention: Librarian | 1 |
| *Sunstrand Aviation<br>2480 West 70th Avenue<br>Denver, Colorado 80221<br>Attention: Librarian | 1 |
| S. V. Manson & Company, Inc.<br>2420 Wilson Boulevard<br>Arlington, Virginia 22201<br>Attention: Librarian | 1 |
| The Bendix Corporation<br>Research Laboratories Division<br>Southfield, Michigan<br>Attention: Librarian | 1 |
| The Boeing Company<br>Aero-Space Division<br>P. O. Box 307, Seattle 25, Washington<br>Attention: Librarian | 1 |
| TRW, Inc.<br>7209 Platt Avenue<br>Cleveland, Ohio 44104<br>Attention: Librarian | 1 |
| Union Carbide Corporation<br>Linde Division<br>61 East Park Drive, Tonowanda, New York<br>Attention: Librarian | 1 |
| United Aircraft Corporation Research Laboratories<br>East Hartford, Connecticut 06108<br>Attention: Librarian | 1 |
| Westinghouse Electric Corporation<br>Astronuclear Laboratory<br>P. O. Box 10864<br>Pittsburgh, Pennsylvania 15236<br>Attention: Librarian | 1 |